arXiv:2412.07626v1 [cs.CV] 10 Dec 2024

OmniDocBench: Benchmarking Diverse PDF Document Parsing with Comprehensive Annotations

Linke Ouyang[1*] Yuan Qu[1*] Hongbin Zhou[1*] Jiawei Zhu[1*] Rui Zhang[1*] Qunshu Lin[2*]
Bin Wang[1*†] Zhiyuan Zhao[1] Man Jiang[1] Xiaomeng Zhao[1] Jin Shi[1] Fan Wu[1] Pei Chu[1] Minghao Liu[3]
Zhenxiang Li[1] Chao Xu[1] Bo Zhang[1] Botian Shi[1] Zhongying Tu[1] Conghui He[1‡]

[1]Shanghai AI Laboratory [2]Abaka AI [3]2077AI

Abstract

Document content extraction is crucial in computer vision, especially for meeting the high-quality data needs of large language models (LLMs) and retrieval-augmented generation (RAG) technologies. However, current document parsing methods suffer from significant limitations in terms of diversity and comprehensive evaluation. To address these challenges, we introduce OmniDocBench, a novel multi-source benchmark designed to advance automated document content extraction. OmniDocBench includes a meticulously curated and annotated high-quality evaluation dataset comprising nine diverse document types, such as academic papers, textbooks, slides, among others. Our benchmark provides a flexible and comprehensive evaluation framework with 19 layout category labels and 14 attribute labels, enabling multi-level assessments across entire datasets, individual modules, or specific data types. Using OmniDocBench, we perform an exhaustive comparative analysis of existing modular pipelines and multimodal end-to-end methods, highlighting their limitations in handling document diversity and ensuring fair evaluation. OmniDocBench establishes a robust, diverse, and fair evaluation standard for the document content extraction field, offering crucial insights for future advancements and fostering the development of document parsing technologies. The codes and dataset is available in https://github.com/opendatalab/OmniDocBench.

1. Introduction

Document parsing is a foundational task in computer vision, focused on accurately extracting content from documents [18, 36, 39, 41, 45]. High-quality document content extraction typically involves the integration of multiple algorithmic modules. Layout detection algorithms identify different content areas on a page, OCR technology converts images of text regions into text, while formula and table recognition models identify specific regions and transform them into corresponding source code. These modules and reading order algorithms form a comprehensive process of converting documents into machine-readable formats.

With large models increasingly requiring high-quality data, the importance of document content extraction has become more pronounced. Although vast amounts of data are available online for training, knowledge-rich document data is relatively scarce. Documents such as academic papers and technical reports contain rich structured information that can significantly enhance the knowledge depth of large models. Moreover, the development of retrieval-augmented generation (RAG) [10, 21] technology relies on extracting accurate information from documents to improve the quality and relevance of generated content. Consequently, research in document content extraction has intensified, leading to a series of pipeline-based high-quality document extraction algorithms [36] and the emergence of end-to-end multimodal large model solutions [3, 5, 6, 27, 39, 40, 42]. These methods have significantly improved document content parsing quality, providing robust support for the needs of large models and RAG technology.

In analyzing current module-based pipeline and multimodal end-to-end methods, we identified several limitations. For instance, methods like Marker and MinerU, which are mainstream pipeline methods, primarily evaluate individual modules on academic paper data, lacking document diversity and comprehensive evaluation results. Although MinerU considers the generalization of diverse data, it only demonstrates this through a single model and visualization results, lacking overall end-to-end evaluation. Multimodal large model methods [3, 5, 27, 39, 40], while easier to use than pipeline methods, lack performance validation on diverse documents, and some evaluation metrics are in-

* The authors contributed equally.
† Project lead.
‡ Corresponding author (heconghui@pjlab.org.cn).

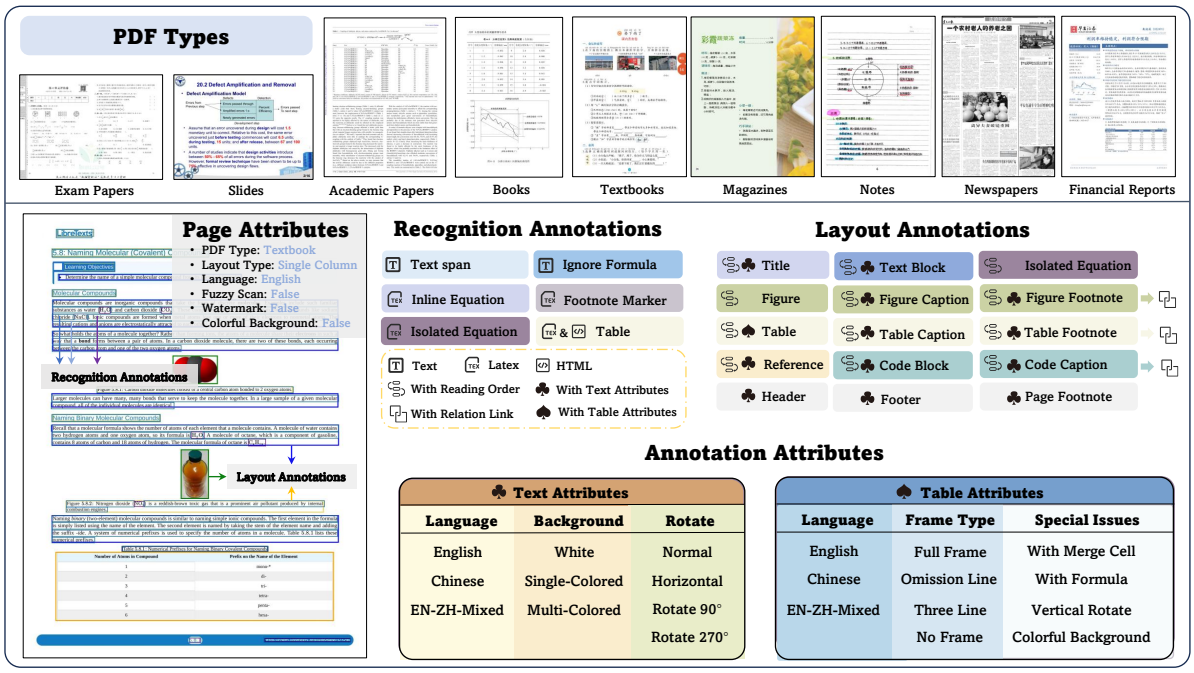

Figure 1. OmniDocBench Data Diversity. It contains 9 PDF page types, along with Layout Annotations and Recognition Annotations. Furthermore, there are 5 Page Attributes, 3 Text Attributes, and 6 Table Attributes.

adequate. Additionally, these methods often use data similar to their training set distribution for comparison, resulting in unfair evaluations. **Overall, current document content extraction faces the following challenges:**

- **Limited document types**. Current evaluations mostly focus on a single type of academic paper, while real-world scenarios include textbooks, exam papers, financial reports, newspapers, magazines, and other document types.
- **Monotonous evaluation dimensions**. Pipeline-based methods typically evaluate specific algorithmic modules, such as OCR, layout detection, or formula recognition, while the overall quality of parsing results requires comprehensive metrics.
- **Inadequate evaluation metrics**. Multimodal large model approaches attempt to evaluate document parsing quality across multiple dimensions, such as dividing document content into text, formulas, tables, etc. However, these models commonly employ evaluation metrics such as BLEU scores or Edit distances, which fail to accurately and fairly assess parsing effectiveness when dealing with markup languages like LaTeX or HTML that allow diverse syntactic expressions.

Building a diverse, comprehensive, and accurate evaluation system poses significant challenges, requiring diverse and high-quality data annotation and reasonable evaluation metrics. While READOC extends the evaluation scope to include GitHub README files based on Nougat, there remains a substantial gap in real-world diversity, and the evaluation dimensions lack consideration of attributes. In contrast, this paper proposes a document content extraction benchmark, **OmniDocBench**, characterized by diverse types, detailed annotations, and reasonable evaluation (Figure 1). **The specific contributions are as follows:**

- **High-quality, diverse evaluation set**: Through automated annotation, manual verification, and expert review, we construct a comprehensive, detailed, high-quality OmniDocBench evaluation set, encompassing nine types of diverse document pages, including papers, textbooks, exam questions, and research reports.
- **Flexible and comprehensive evaluation dimension support**: The OmniDocBench validation set covers 19 layout category labels and 14 attribute labels. To facilitate user evaluation from an overall, single module, or different data types, we provide end-to-end evaluation, single algorithm module evaluation, and attribute-based evaluation, covering various evaluation needs.
- **Comprehensive evaluation of mainstream methods**: Based on OmniDocBench, we conduct a comprehensive evaluation of current mainstream modular pipeline and end-to-end large model methods, providing a fairer assessment of existing methods and summarizing the shortcomings of current document parsing methods, thereby guiding further development in document parsing.

2. Related Work

2.1. Traditional Document Content Extraction

Document Content extraction remains a challenging task, and there is yet to emerge a unified benchmark tailored for

Benchmark	Document Categories	Annotaion Type					Single-Module Eval				End-to-End Eval			
		BBox	Text	Table	Order	Formula	OCR	DLA	TR	MFR	OCR	ROD	TR	MFR
Single-Module Eval Benchmark														
Robust Reading [19]	1	✔				✔								
PubLayNet [43], DocBank [24], DocLayNet [31], M^{6}Doc [7]	1, 1, 5, 6	✔					✔							
PubTabNet [47],TableX [9], TableBank [23]	1, 1, 1			✔				✔						
Im2Latex-100K [8],UniMER-Test [34]	1				✔					✔				
End-to-end Eval Benchmarks														
Nougat [5]	1		✔								✔	✔	✔	✔
Fox [27]	2		✔								✔			
GOT OCR 2.0 [39]	2		✔								✔		✔	✔
READoc [26]	2		✔	✔	✔	✔					✔	✔	✔	✔
OmniDocBench	9	✔	✔	✔	✔	✔	✔	✔	✔	✔	✔	✔	✔	✔

Table 1. A comparison between OmniDocBench and existing DCE benchmarks. *OCR*: Optical Character Recognition; *DLA*: Document Layout Analysis; *MFR*: Math Formula Recognition; *TR*: Table Recognition; *ROD*: Reading Order Detection

real-world scenarios. Traditional algorithms typically employ multiple expert modules to handle different extraction subtasks, such as document layout detection [11, 16, 32, 46], optical character recognition (OCR) [14, 22, 28, 33, 37], formula recognition [4, 25, 34, 44], and table recognition [15, 17, 22].

While expert models of these subtasks are advancing rapidly, recent work such as Mineru [36] attempts to concatenate multiple expert modules into a pipeline and provides a high-precision open-source solution for document content extraction. READOC [26] also unifies heterogeneous evaluation methods from the perspective of Document Structure Extraction, breaking down texts, images, formulas, tables, and other dimensions for evaluation, thus offering a solution-oriented towards real-world scenarios for DSE tasks. However, due to the complexity of Document data sources and the intricacies of PDF document information, previous efforts still fall short in terms of data diversity, failing to cover the categories users encounter in practical applications. Similarly, there is an issue with the explainability of document parsing.

2.2. VLM-based Document Content Extraction

The emergence of Vision-Language Models (VLMs) [1, 6, 12, 38] has revolutionized the field of document content extraction. These models leverage multi-modality capability to achieve remarkable performance in document understanding tasks. Document extraction tools powered by VLMs excel at comprehending both visual layouts and textual content, effectively handling complex document structures while capturing rich contextual information. Representative works such as Nougat [5], Vary [40], Fox [27], and GOT [39], along with recent advances [13, 29], demonstrate significant progress in automated document parsing and comprehension. Despite these advances, the field lacks a standardized and unified benchmark for evaluating VLM-based document extraction task. This absence has hindered objective assessment of PDF document processing capabilities and impeded fair comparison across different approaches. To address this limitation, we present OmniDocBench, a comprehensive end-to-end benchmark designed specifically for evaluating VLM-based document parsing in real-world scenarios.

2.3. Benchmark for Document Content Extraction

An end-to-end benchmark for PDFs can intuitively reflect the effectiveness of PDF extraction tools, which is crucial for their iteration and selection. However, current benchmarks predominantly focus on module-level evaluations; we have listed related benchmarks in Table 1. Additionally, while there are existing end-to-end benchmarks, they lack detailed annotation rules and suffer from insufficient diversity, as well as unreasonable metrics for formula and table evaluations. For example, READOC [26] covers only two types of sources—arXiv and GitHub—and uses EDS [20] and TEDS [47] to compute metrics for formulas and tables, which may lead to inaccuracies CDM [35]. Therefore, there is a need for a more finely annotated, diverse, and reasonably evaluated end-to-end benchmark.

3. OmniDocBench Dataset

Constructing a diverse and comprehensive document parsing benchmark with precise annotations is a formidable challenge. As illustrated in Figure 2, we have designed a systematic and professional annotation framework for OmniDocBench, encompassing data acquisition, intelligent pre-annotation, and manual refinement. This ensures that OmniDocBench possesses the following key attributes:

- **Page Diversity**. We sourced document pages from a variety of origins to ensure a wide range of document types.
- **Comprehensive Annotation**. We meticulously anno-

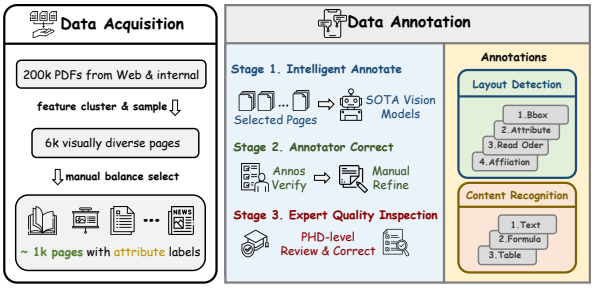

Figure 2. Overview of the OmniDocBench dataset construction.

tated all elements on the pages, including bounding boxes, specific content, and various potential attributes.

- **Annotation Accuracy**. By integrating semi-automated annotation processes, annotator corrections, and expert quality checks, we ensure the reliability of all annotations.

The following sections detail the data acquisition process, the annotation methodology, and a statistical analysis of the final annotated dataset.

3.1. Data Acquisition

During the data acquisition phase, we sourced document pages from diverse origins and used clustering algorithms to initially select visually diverse pages, followed by manual annotation of page attributes to finalize the OmniDocBench pages. Specifically, we collected 200,000 initial PDF documents from Common Crawl, Google, Baidu search engines, and internal data. Subsequently, we extracted visual features from these document pages using ResNet-50 and performed clustering using Faiss [1], sampling 6,000 visually diverse pages from 10 cluster centers. Finally, annotators provided page-level attribute annotations, including page type, layout type, and language type, and further balanced the selection to 981 samples for the final dataset. The OmniDocBench dataset includes pages with 9 types of pages, multiple layout categories, and various attribute annotations, covering a wide range of real-world scenarios.

3.2. Data Annotation

To ensure the comprehensiveness of OmniDocBench's annotations, we conducted detailed annotations for layout detection and content recognition.

3.2.1. Annotation Types

Layout Detection Annotations: Unlike typical layout detection tasks, OmniDocBench includes four comprehensive types of annotations: (1) Layout Bounding Box Annotations: Locating information for 19 types of regions such as titles, text paragraphs, tables, and images. (2) Layout Attribute Annotations: Detailed attribute annotations for detected boxes, including 3 text box attributes, 6 table attributes, and 2 formula attributes. (3) Reading Order Annotations: Annotating the reading sequence of detected boxes. (4) Affiliation Annotations: For images, tables, formulas, and code blocks, we annotate captions and titles to distinguish them from main text. Similarly, for cross-page paragraphs, we annotate affiliation relationships.

Content Recognition Annotations: Based on the format of the content area, we conduct the following three types of area annotations: (1) Text Annotations: Pure text annotations for titles, text paragraphs, and other plain text content. (2) Formula Annotations: LaTeX format annotations for inline formulas, display formulas, and subscripts. (3) Table Annotations: Providing both HTML and LaTeX annotations for table data.

3.2.2. Annotation Process

For these annotation tasks on diverse pages, we design a standardized process to ensure quality and efficiency, comprising intelligent pre-annotation, annotator correction, and expert quality inspection.

Intelligent Pre-Annotation. Manually annotating entire documents is time-consuming and costly. To enhance efficiency, we employ state-of-the-art detection and recognition models for pre-annotation of layout detection and content recognition. Specifically, we use fine-tuned LayoutLMv3 [16] for layout detection annotations and PaddleOCR [22], UniMERNet [34], and GPT-4o [2] for text, formula, and table annotations, respectively.

Annotator Correction. After layout detection phase, annotators refine the detection boxes and enhance annotations with reading order and affiliation details. Each character is verified to ensure accuracy in content recognition. For complex annotations of tables and formulas, requiring LaTeX and HTML formats, annotators use tools like Tables Generator [2] and latexlive [3] for verification and correction.

Expert Quality Inspection. Despite thorough annotator corrections, the complexity of formulas and tables may result in residual issues. To address these, we use CDM's rendering techniques to identify unrenderable elements. These are then reviewed and corrected by three researchers to ensure accuracy and fidelity in the final annotations.

3.3. Dataset Statistics

Page Diversity. OmniDocBench comprises a total of 981 PDF pages across 9 distinct types. Each page is annotated with global attributes, including text language, column layout type, and indicators for blurred scans, watermarks, and colored backgrounds.

Annotation Diversity: OmniDocBench contains over 10,0000 annotations for page detection and recognition: (1)

[1] https://github.com/facebookresearch/faiss

[2] https://www.tablesgenerator.com/

[3] https://www.latexlive.com/

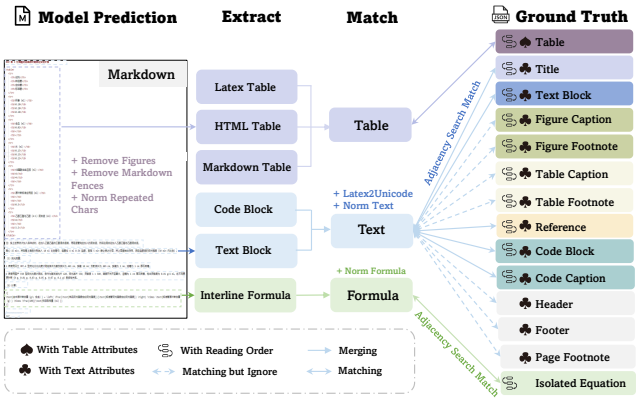

Figure 3. OmniDocBench Evaluation Pipeline.

More than 20,000 block-level annotations across 15 categories, including over 9,000 text paragraphs, 989 image boxes, 428 table boxes, and so on. All document components except headers, footers, and page notes are labeled with reading order information, totaling over 16,000 annotations. (2) The dataset also includes more than 80,000 span-level annotations across four categories, with 4,000 inter-line formulas and footnote markers represented in LaTeX format, while the remaining annotations are in text format.

Annotation Attribute Diversity: (1) *Text Attributes:* All block-level annotations, except for tables and images, include text attribute tags. In addition to standard Chinese and English text, there are over 2,000 blocks with complex backgrounds and 146 with rotated text. (2) *Table Attributes:* Besides standard Chinese and English tables, there are 142 with complex backgrounds, 81 containing formulas, 150 with merged cells, and 7 vertical tables.

4. OmniDocBench Evaluation Methodology

To provide a fair and comprehensive evaluation for various models, we proposed an end-to-end evaluation pipeline consisting of several modules, including extraction, matching algorithm, and metric calculation, as shown in Figure 3. It ensures that OmniDocBench automatically performs unified evaluation on end-to-end DCE tasks, thereby producing reliable and effective evaluation results.

4.1. Extraction

Preprocessing: The model-generated markdown text should be preprocessed, which includes removing images, eliminating markdown tags at the beginning of the document, and standardizing the number of repeated characters.

Special Component Extraction: Extraction is primarily carried out using regular expression matching. To ensure that the extraction of content does not interfere with each other, it is necessary to follow a specific order. The extraction sequence is as follows: LaTeX tables, HTML tables, display formulas, markdown tables (which are then converted into HTML format), and code blocks.

Pure Text Extraction: After extracting special components, the remaining content is considered pure text. Paragraphs are separated by double line breaks, allowing them to participate in subsequent matching processes, thus aligning with reading order annotation units in the GTs. If no double line break exists, single line breaks are used for paragraph separation. Additionally, previously extracted code blocks are merged into the text category for processing.

Inline Formula Format Converting: We standardized inline formulas within paragraphs to Unicode format. This was necessary because different models produce inconsistent outputs for inline formulas. For formulas originally written in Unicode, it is hard to extract them using regular expressions. Therefore, to ensure a fair comparison, we do not extract inline formulas for separate evaluation. Instead, we include them in their Unicode format alongside the text paragraphs for evaluation.

Reading Order Extraction: Upon completion of the extraction, the start and end positions of the extracted content in the original markdown are recorded for subsequent reading order calculation.

4.2. Matching Algorithm

To avoid the impact of paragraph splitting on the final results, we proposed a method, Adjacency Search Match, that merges and splits paragraphs in both GTs and Preds to achieve the best possible match. The specific strategy involves: i) Calculate a metrix of Normalized Edit Distance between GTs and Preds. If the similarity between a Pred and a GT exceeds a specific threshold, they are considered a successful match. ii) For the rest, we apply fuzzy matching to determine whether one string is a subset of another string. If so, we further apply the truncation and merging algorithm which would try to merge adjacent paragraph. This process would continue to merge more paragraph until the Normalized Edit Distance starts to decrease. After this process, the best match will be found for GTs and Preds.

4.3. Metric Calculation

Ignore Handling: We implement an ignore logic for certain components in PDF page content, meaning they participate in matching but are excluded from metric calculations. This is mainly because of inconsistent output standards among models, which should not affect the validation results. For fairness, we ignore: (1) Headers, footers, page numbers, and page footnotes, which are handled inconsistently by different models. (2) Captions for figures, tables, and footnotes often have uncertain placement, complicating reading order. Additionally, some models embed table captions in HTML or LaTeX tables, while others treat them as plain text.

Method Type	Methods	Text$^{Edit}\downarrow$		Formula$^{Edit}\downarrow$		Formula$^{CDM}\uparrow$		Table$^{TEDS}\uparrow$		Table$^{Edit}\downarrow$		Read Order$^{Edit}\downarrow$		Overall$^{Edit}\downarrow$	
		EN	*ZH*	*EN*	*ZH*	*EN*	*ZH*	*EN*	*ZH*	*EN*	*ZH*	*EN*	*ZH*	*EN*	*ZH*
Pipeline Tools	MinerU	**0.058**	**0.211**	**0.278**	0.577	66.9	49.5	**79.4**	62.7	**0.305**	0.461	**0.079**	0.288	**0.180**	0.384
	Marker	0.141	0.303	0.667	0.868	18.4	12.7	54.0	45.8	0.718	0.763	0.138	0.306	0.416	0.560
	Mathpix	0.101	0.358	0.306	**0.454**	71.4	**72.7**	77.9	**68.2**	0.322	**0.416**	0.105	0.275	0.209	**0.376**
Expert VLMs	GOT-OCR	0.187	0.315	0.360	0.528	**81.8**	51.4	53.5	48.0	0.521	0.594	0.141	0.28	0.302	0.429
	Nougat	0.365	0.998	0.488	0.941	17.4	16.9	40.3	0.0	0.622	1.000	0.382	0.954	0.464	0.973
General VLMs	GPT4o	0.144	0.409	0.425	0.606	76.4	48.2	72.8	63.7	0.363	0.474	0.128	0.251	0.265	0.435
	Qwen2-VL	0.252	0.251	0.468	0.572	54.9	60.9	59.9	66.8	0.591	0.587	0.255	**0.223**	0.392	0.408
	InternVL2	0.353	0.290	0.543	0.701	69.8	49.6	63.8	61.1	0.616	0.638	0.317	0.228	0.457	0.464

Table 2. Comprehensive evaluation of document parsing algorithms on OmniDocBench: performance metrics for text, formula, table, and reading order extraction, with overall scores derived from ground truth comparisons.

Model Type	Models	Book	Slides	Financial Report	Textbook	Exam Paper	Magazine	Academic Papers	Notes	Newspaper	Average
Pipeline Tools	MinerU	**0.044**	0.124	**0.033**	**0.102**	**0.159**	0.072	**0.025**	0.984	**0.148**	**0.188**
	Marker	0.188	0.327	0.087	0.292	0.423	0.134	0.102	0.470	0.270	0.255
	Mathpix	0.131	0.168	0.202	0.199	0.278	0.138	0.091	0.631	0.648	0.276
Expert VLMs	GOT-OCR	0.105	0.222	0.067	0.132	0.204	0.198	0.179	0.388	0.771	0.252
	Nougat	0.734	0.958	1.000	0.820	0.930	0.83	0.214	0.991	0.871	0.816
General VLMs	GPT4o	0.157	0.163	0.348	0.187	0.281	0.173	0.146	0.607	0.751	0.313
	Qwen2-VL	0.094	**0.08**	0.145	0.148	0.219	**0.065**	0.315	0.298	0.79	0.239
	InternVL2	0.216	0.098	0.162	0.184	0.247	0.150	0.419	**0.226**	0.903	0.289

Table 3. End-to-end text recognition performance on OmniDocBench: evaluation using edit distance **across 9 PDF page types**.

Models	Fuzzy	Water	Color	Mean	Variance
Pipeline Tools					
MinerU	0.15	**0.151**	**0.107**	0.136	0.0004
Marker	0.286	0.436	0.290	0.337	0.0049
Mathpix	0.294	0.290	0.182	0.255	0.0027
Expert VLMs					
GOT-OCR	0.175	0.190	0.186	0.184	**0.0000**
Nougat	0.934	0.915	0.873	0.907	0.0006
General VLMs					
GPT4o	0.263	0.195	0.184	0.214	0.0012
Qwen2-VL	**0.101**	0.157	0.114	**0.124**	0.0006
InternVL2	0.120	0.197	0.155	0.157	0.0010

Table 4. End-to-end text recognition on OmniDocBench: evaluation **under various page attributes** using the edit distance metric. Columns represent: Fuzzy (Fuzzy scan), Water (Watermark), Color (Colorful background).

Models	Single	Double	Three	Complex	Mean	Variance
Pipeline Tools						
MinerU	0.311	**0.101**	**0.117**	**0.376**	**0.226**	0.0143
Marker	0.231	0.251	0.309	0.378	0.292	**0.0033**
Mathpix	0.189	0.175	0.225	0.413	0.250	0.0091
Expert VLMs						
GOT-OCR	0.163	0.145	0.257	0.468	0.258	0.0165
Nougat	0.852	0.601	0.662	0.873	0.747	0.0139
General VLMs						
GPT4o	0.109	0.204	0.254	0.426	0.248	0.0132
Qwen2-VL	0.098	0.248	0.517	0.429	0.323	0.0263
InternVL2	**0.082**	0.312	0.682	0.444	0.380	0.0472

Table 5. End-to-end reading order evaluation on OmniDocBench: results **across different column layout types** using Normalized Edit Distance.

Metric: Different calculation methods are used for various document components: (1) **Pure Text:** We calculate Normalized Edit Distance, averaging these metrics at the sample level to obtain the final scores. (2) **Tables:** All tables are converted to HTML format before calculating the TEDS metric and Normalized Edit Distance. (3) **Formulas:** Formulas are currently evaluated using the CDM [35], Normalized Edit Distance, and BLEU. We did not convert interline formulas into Unicode because Unicode cannot represent certain complex formulas, such as matrices. (4) **Reading Order:** Reading order use the Normalized Edit Distance as metric. It only involves text components, where tables, images, and ignored components do not participate in the final reading order calculation.

5. Benchmarks

5.1. Component-specific Evaluation Results

The OmniDocBench dataset features comprehensive and precise annotations, allowing for a fair and rigorous comparison of various document content extraction algorithms in real-world scenarios. Based on the distinct characteristics of these algorithms, we categorize document content

Model	Book	Slides	Research Report	Textbook	Exam Paper	Magazine	Academic Literature	Notes	Newspaper	Average mAP
DiT-L	43.44	13.72	45.85	15.45	3.40	29.23	66.13	0.21	23.65	26.90
LayoutLMv3	42.12	13.63	43.22	21.00	5.48	31.81	64.66	0.80	30.84	28.84
DOCX-Chain	30.86	11.71	39.62	19.23	10.67	23.00	41.60	1.80	16.96	21.27
DocLayout-YOLO	**43.71**	**48.71**	**72.83**	**42.67**	**35.40**	**51.44**	**66.84**	**9.54**	**57.54**	**48.71**

Table 6. Component-level layout detection evaluation on OmniDocBench layout subset: mAP results by PDF page type.

Model Type	Model	Language			Table Frame Type				Special Situation				Overall
		EN	*ZH*	*Mixed*	*Full*	*Omission*	*Three*	*Zero*	*Merge Cell*(+/-)	*Formula*(+/-)	*Colorful*(+/-)	*Rotate*(+/-)	
OCR-based Models	PaddleOCR	76.8	71.8	80.1	67.9	74.3	81.1	74.5	70.6/75.2	71.3/74.1	72.7/74.0	23.3/74.6	73.6
	RapidTable	**80.0**	**83.2**	**91.2**	**83.0**	**79.7**	**83.4**	78.4	**77.1/85.4**	**76.7/83.9**	**77.6/84.9**	25.2/83.7	**82.5**
Expert VLMs	StructEqTable	72.0	72.6	81.7	68.8	64.3	80.7	**85.0**	65.1/76.8	69.4/73.5	66.8/75.7	**44.1/73.3**	72.7
	GOT-OCR	72.2	75.5	85.4	73.1	72.7	78.2	75.7	65.0/80.2	64.3/77.3	70.8/76.9	8.5/76.3	74.9
General VLMs	Qwen2-VL-7B	70.2	70.7	82.4	70.2	62.8	74.5	80.3	60.8/76.5	63.8/72.6	71.4/70.8	20.0/72.1	71.0
	InternVL2-8B	70.9	71.5	77.4	69.5	69.2	74.8	75.8	58.7/78.4	62.4/73.6	68.2/73.1	20.4/72.6	71.5

Table 7. Component-level Table Recognition evaluation on OmniDocBench table subset. *(+/-)* means *with/without* special situation.

extraction methods into three main classes:

Pipeline Tools. These methods integrate layout detection and various content recognition tasks (such as OCR, table recognition, and formula recognition) into a document parsing pipeline for content extraction. Prominent examples include MinerU [36], Marker [30], and Mathpix [4].

Expert VLMs. These are large multimodal models specifically trained for document parsing tasks. Representative models include GOT-OCR2.0 [39] and Nougat [5].

General VLMs. These are general-purpose large multimodal models inherently capable of document parsing. Leading models in this category include GPT-4o [2], Qwen2-VL [38], and InternVL2 [6].

5.2. End-to-End Evaluation Results

Utilizing the OmniDocBench dataset and our evaluation framework, we conducted end-to-end assessments of mainstream document parsing methods, evaluating their performance from input PDF images to the resultant document parsing outputs.

Overall Evaluation Results. As illustrated in Table 2, pipeline tools specifically designed for document parsing, demonstrate superior performance across the board. MinerU and Mathpix achieved the best results for English and Chinese pages, respectively. In contrast, even the best general-purpose Vision Language Models (VLMs), GPT-4o, exhibits a performance gap compared to these specialized models, especially in Chinese. This trend is evident across sub-tasks like text recognition, formula recognition, and table recognition, where methods tailored for document parsing consistently outperform others. This advantage is largely due to the fine-tuning of these models on large datasets specific to document parsing tasks.

[4] https://mathpix.com/

Performance Across Diverse Page Types. To gain deeper insights into model performance on diverse document types, we evaluated text recognition tasks across different page types. As shown in Table 3, an intriguing finding emerged: For commonly used data, such as academic papers and financial reports, pipeline tools perform well. However, for more specialized data like slides and handwritten notes, general VLMs demonstrate stronger generalization. The reason is clear: Pipeline tools and expert VLMs are relatively more constrained by the range of training data, whereas general VLMs having been trained on a wide variety of samples, maintained excellent recognition performance even in traditionally challenging long-tail scenarios, underscoring the value of VLMs.

Performance on Pages with Specific Attributes. For documents in OmniDocBench with attributes such as fuzzy scans, watermarks, and colorful backgrounds, our evaluation results are presented in Table 4. In these scenarios, the VLMs InternVL2 and Qwen2-VL exhibit the strongest resistance to interference, achieving the best accuracy and robustness. MinerU also performs commendably.

Performance on Different Column Layout Types. OmniDocBench annotates page attributes such as column layout type, which is crucial for analyzing model performance in reading order. As depicted in Table 5, all models experience a noticeable decline in reading order accuracy when dealing with complex layouts. MinerU and Mathpix excels in reading order across various column layouts, demonstrating robust performance across different page types.

From these end-to-end evaluations, it is evident that pipeline tools like MinerU and Mathpix, specifically designed for document parsing, achieve the best overall performance. However, in terms of versatility and scalability, VLMs offer a distinct advantage over pipeline tools. Fine-

Model Type	Model	Language			Text background			Text Rotate			
		EN	*ZH*	*Mixed*	*White*	*Single*	*Multi*	*Normal*	*Rotate90*	*Rotate270*	*Horizontal*
Expert Vision Models	PaddleOCR	0.071	**0.055**	**0.118**	**0.060**	**0.038**	**0.085**	**0.060**	**0.015**	0.285	**0.021**
	Tesseract OCR	0.179	0.553	0.553	0.453	0.463	0.394	0.448	0.369	0.979	0.982
	Surya	0.057	0.123	0.164	0.093	0.186	0.235	0.104	0.634	0.767	0.255
	GOT-OCR	0.041	0.112	0.135	0.092	0.052	0.155	0.091	0.562	0.966	0.097
	Mathpix	0.033	0.240	0.261	0.185	0.121	0.166	0.180	0.038	**0.185**	0.638
Vision Language Models	Qwen2-VL	0.072	0.274	0.286	0.234	0.155	0.148	0.223	0.273	0.721	0.067
	InternVL2	0.074	0.155	0.242	0.113	0.352	0.269	0.132	0.610	0.907	0.595
	GPT4o	**0.020**	0.224	0.125	0.167	0.140	0.220	0.168	0.115	0.718	0.132

Table 8. Component-level evaluation on OmniDocBench OCR subset: results grouped by text attributes using the edit distance metric.

Models	CDM	ExpRate@CDM	BLEU	Norm Edit
GOT-OCR	74.1	28.0	55.07	0.290
Mathpix	86.6	2.8	**66.56**	0.322
Pix2Tex	73.9	39.5	46.00	0.337
UniMERNet-B	85.0	60.2	60.84	**0.238**
GPT4o	**86.8**	**65.5**	45.17	0.282
InternVL2	67.4	54.5	47.63	0.308
Qwen2-VL	83.8	55.4	53.71	0.285

Table 9. Component-level formula recognition evaluation on OmniDocBench formula subset.

tuning a general large model like Qwen2-VL with specialized data could yield models even more adept at document parsing, indicating a promising direction for future research in multimodal approaches.

The OmniDocBench dataset provides comprehensive annotations for document parsing, including layout detection, text boxes and content, formula boxes and content, and table boxes and content. These detailed annotations enable the evaluation of current state-of-the-art (SOTA) methods across various document types, allowing us to analyze their performance in diverse scenarios. Additionally, these results can be used to assemble enhanced pipeline tools for document parsing tasks.

5.3. Single Algorithm Evaluation Results

Layout Detection Results. Layout detection is the first step in document parsing using pipeline tools. A robust layout detection algorithm should perform well across a variety of document types. Table 6 presents an evaluation of leading layout detection models. The DocLayout-YOLO method, which is pre-trained on diverse synthetic document data, significantly outperforms other approaches. This superiority is a key factor in MinerU's integration of DocLayout-YOLO, contributing to its outstanding overall performance. The table also reveals that, aside from DocLayout-YOLO, other methods perform well on books and academic literature but are less effective on other document types, primarily due to a lack of pre-training on diverse documents.

Table Recognition Results. Table recognition results evaluated by Tree-Edit-Distance-based Similarity (TEDS) metric are presented in Table 7. We evaluate table recognition models across three dimensions on our OmniDocBench table subset: language diversity, table frame types, and special situations. Among all models, OCR-based models demonstrate superior overall performance, with RapidTable achieving the highest scores in language diversity and maintaining stable performance across different frame types. Expert VLMs show competitive results in specific scenarios, with StructEqTable [48] excelling in no frame tables and showing better rotation robustness. General VLMs (Qwen2-VL-7B and InternVL2-8B) exhibit relatively lower but consistent performance, suggesting that while general-purpose VLMs have made progress in table understanding, they still lag behind specialized solutions.

Text Recognition Results. In the traditional OCR task, Table 8 shows that PaddleOCR leads the field, surpassing other models significantly, with GOT also performing relatively well. Selecting these two methods for the OCR module is a prudent choice.

Formula Recognition Results. For formula recognition, the CDM metric provides a clear comparison in Table 9. GPT-4o, Mathpix, and UniMERNet achieve results of 86.8%, 86.6%, and 85.0%, respectively. Notably, GPT-4o excels with a recall rate of 65.5% under strict conditions requiring perfect character accuracy. Although Mathpix shows high character-level precision, it occasionally omits punctuation, such as commas, leading to a lower overall correctness rate. Nonetheless, all three models are strong candidates for formula recognition tasks.

6. Conclusion

This paper addresses the lack of diverse and realistic benchmarks in document parsing research by introducing OmniDocBench, a dataset featuring a variety of page types with comprehensive annotations, along with a flexible and reliable evaluation framework. OmniDocBench enables systematic and fair assessments of document parsing methods, providing crucial insights for advancing the field. Its task-specific and attribute-level evaluations facilitate targeted model optimization, promoting more robust and effective parsing solutions.

References

[1] Josh Achiam, Steven Adler, Sandhini Agarwal, Lama Ahmad, Ilge Akkaya, Florencia Leoni Aleman, Diogo Almeida, Janko Altenschmidt, Sam Altman, Shyamal Anadkat, et al. Gpt-4 technical report. *arXiv:2303.08774*, 2023. 3

[2] Open AI. Hello gpt 4o, 2024. Accessed July 24, 2024. 4, 7

[3] Jinze Bai, Shuai Bai, Shusheng Yang, Shijie Wang, Sinan Tan, Peng Wang, Junyang Lin, Chang Zhou, and Jingren Zhou. Qwen-vl: A versatile vision-language model for understanding, localization, text reading, and beyond. *arXiv:2308.12966*, 2024. 1

[4] Lukas Blecher. pix2tex - latex ocr. https://github.com/lukas-blecher/LaTeX-OCR, 2022. Accessed: 2024-2-29. 3

[5] Lukas Blecher, Guillem Cucurull, Thomas Scialom, and Robert Stojnic. Nougat: Neural optical understanding for academic documents. *arXiv:2308.13418*, 2024. 1, 3, 7

[6] Zhe Chen, Jiannan Wu, Wenhai Wang, Weijie Su, Guo Chen, Sen Xing, Muyan Zhong, Qinglong Zhang, Xizhou Zhu, Lewei Lu, Bin Li, Ping Luo, Tong Lu, Yu Qiao, and Jifeng Dai. Internvl: Scaling up vision foundation models and aligning for generic visual-linguistic tasks. In *Proceedings of the IEEE/CVF Conference on Computer Vision and Pattern Recognition*, pages 24185–24198, 2024. 1, 3, 7

[7] Hiuyi Cheng, Peirong Zhang, Sihang Wu, Jiaxin Zhang, Qiyuan Zhu, Zecheng Xie, Jing Li, Kai Ding, and Lianwen Jin. M6doc: A large-scale multi-format, multi-type, multi-layout, multi-language, multi-annotation category dataset for modern document layout analysis. In *Proceedings of the IEEE/CVF Conference on Computer Vision and Pattern Recognition*, pages 15138–15147, 2023. 3

[8] Yuntian Deng, Anssi Kanervisto, Jeffrey Ling, and Alexander M Rush. Image-to-markup generation with coarse-to-fine attention. In *International Conference on Machine Learning*, pages 980–989. PMLR, 2017. 3

[9] Harsh Desai, Pratik Kayal, and Mayank Singh. Tablex: a benchmark dataset for structure and content information extraction from scientific tables. In *Document Analysis and Recognition–ICDAR 2021: 16th International Conference*, pages 554–569, 2021. 3

[10] Yunfan Gao, Yun Xiong, Xinyu Gao, Kangxiang Jia, Jinliu Pan, Yuxi Bi, Yi Dai, Jiawei Sun, Meng Wang, and Haofen Wang. Retrieval-augmented generation for large language models: A survey. *arXiv:2312.10997*, 2023. 1

[11] Jiuxiang Gu, Jason Kuen, Vlad I Morariu, Handong Zhao, Rajiv Jain, Nikolaos Barmpalios, Ani Nenkova, and Tong Sun. Unidoc: Unified pretraining framework for document understanding. *Advances in Neural Information Processing Systems*, 34:39–50, 2021. 3

[12] Anwen Hu, Haiyang Xu, Jiabo Ye, Ming Yan, Liang Zhang, Bo Zhang, Chen Li, Ji Zhang, Qin Jin, Fei Huang, et al. mplug-docowl 1.5: Unified structure learning for ocr-free document understanding. *arXiv preprint arXiv:2403.12895*, 2024. 3

[13] Anwen Hu, Haiyang Xu, Liang Zhang, Jiabo Ye, Ming Yan, Ji Zhang, Qin Jin, Fei Huang, and Jingren Zhou. mplug-docowl2: High-resolution compressing for ocr-free multi-page document understanding. *arXiv preprint arXiv:2409.03420*, 2024. 3

[14] Mingxin Huang, Yuliang Liu, Zhenghao Peng, Chongyu Liu, Dahua Lin, Shenggao Zhu, Nicholas Yuan, Kai Ding, and Lianwen Jin. Swintextspotter: Scene text spotting via better synergy between text detection and text recognition. In *proceedings of the IEEE/CVF conference on computer vision and pattern recognition*, pages 4593–4603, 2022. 3

[15] Xin Huang, Ashish Khetan, Milan Cvitkovic, and Zohar Karnin. Tabtransformer: Tabular data modeling using contextual embeddings. arxiv 2020. *arXiv preprint arXiv:2012.06678*, 2012. 3

[16] Yupan Huang, Tengchao Lv, Lei Cui, Yutong Lu, and Furu Wei. Layoutlmv3: Pre-training for document ai with unified text and image masking, 2022. 3, 4

[17] Yongshuai Huang, Ning Lu, Dapeng Chen, Yibo Li, Zecheng Xie, Shenggao Zhu, Liangcai Gao, and Wei Peng. Improving table structure recognition with visual-alignment sequential coordinate modeling. In *Proceedings of the IEEE/CVF Conference on Computer Vision and Pattern Recognition*, pages 11134–11143, 2023. 3

[18] Wonseok Hwang, Jinyeong Yim, Seunghyun Park, Sohee Yang, and Minjoon Seo. Spatial dependency parsing for semi-structured document information extraction. In *Findings of the Association for Computational Linguistics: ACL-IJCNLP*, pages 330–343. Association for Computational Linguistics (ACL), 2021. 1

[19] Dimosthenis Karatzas, Lluis Gomez-Bigorda, Anguelos Nicolaou, Suman Ghosh, Andrew Bagdanov, Masakazu Iwamura, Jiri Matas, Lukas Neumann, Vijay Ramaseshan Chandrasekhar, Shijian Lu, Faisal Shafait, Seiichi Uchida, and Ernest Valveny. Icdar 2015 competition on robust reading. In *2015 13th International Conference on Document Analysis and Recognition*, pages 1156–1160, 2015. 3

[20] Vladimir I Levenshtein et al. Binary codes capable of correcting deletions, insertions, and reversals. In *Doklady Physics*, pages 707–710. Soviet Union, 1966. 3

[21] Patrick Lewis, Ethan Perez, Aleksandra Piktus, Fabio Petroni, Vladimir Karpukhin, Naman Goyal, Heinrich Küttler, Mike Lewis, Wen-tau Yih, Tim Rocktäschel, et al. Retrieval-augmented generation for knowledge-intensive nlp tasks. *Advances in Neural Information Processing Systems*, 33:9459–9474, 2020. 1

[22] Chenxia Li, Weiwei Liu, Ruoyu Guo, Xiaoting Yin, Kaitao Jiang, Yongkun Du, Yuning Du, Lingfeng Zhu, Baohua Lai, Xiaoguang Hu, Dianhai Yu, and Yanjun Ma. Pp-ocrv3: More attempts for the improvement of ultra lightweight ocr system, 2022. 3, 4

[23] Minghao Li, Lei Cui, Shaohan Huang, Furu Wei, Ming Zhou, and Zhoujun Li. Tablebank: Table benchmark for image-based table detection and recognition. In *Proceedings of the Twelfth Language Resources and Evaluation Conference*, pages 1918–1925, 2020. 3

[24] Minghao Li, Yiheng Xu, Lei Cui, Shaohan Huang, Furu Wei, Zhoujun Li, and Ming Zhou. Docbank: A benchmark dataset for document layout analysis. *arXiv:2006.01038*, 2020. 3

[25] Zhe Li, Lianwen Jin, Songxuan Lai, and Yecheng Zhu. Improving attention-based handwritten mathematical expression recognition with scale augmentation and drop attention. In *2020 17th International Conference on Frontiers in Handwriting Recognition (ICFHR)*, pages 175–180. IEEE, 2020. 3

[26] Zichao Li, Aizier Abulaiti, Yaojie Lu, Xuanang Chen, Jia Zheng, Hongyu Lin, Xianpei Han, and Le Sun. Readoc: A unified benchmark for realistic document structured extraction. *arXiv:2409.05137*, 2024. 3

[27] Chenglong Liu, Haoran Wei, Jinyue Chen, Lingyu Kong, Zheng Ge, Zining Zhu, Liang Zhao, Jianjian Sun, Chunrui Han, and Xiangyu Zhang. Focus anywhere for fine-grained multi-page document understanding. *arXiv:2405.14295*, 2024. 1, 3

[28] Yuliang Liu, Hao Chen, Chunhua Shen, Tong He, Lianwen Jin, and Liangwei Wang. Abcnet: Real-time scene text spotting with adaptive bezier-curve network. In *proceedings of the IEEE/CVF conference on computer vision and pattern recognition*, pages 9809–9818, 2020. 3

[29] Tengchao Lv, Yupan Huang, Jingye Chen, Yuzhong Zhao, Yilin Jia, Lei Cui, Shuming Ma, Yaoyao Chang, Shaohan Huang, Wenhui Wang, Li Dong, Weiyao Luo, Shaoxiang Wu, Guoxin Wang, Cha Zhang, and Furu Wei. Kosmos-2.5: A multimodal literate model, 2024. 3

[30] Vik Paruchuri. Marker, 2024. 7

[31] Birgit Pfitzmann, Christoph Auer, Michele Dolfi, Ahmed S Nassar, and Peter Staar. Doclaynet: A large human-annotated dataset for document-layout segmentation. In *Proceedings of the 28th ACM SIGKDD conference on knowledge discovery and data mining*, pages 3743–3751, 2022. 3

[32] Subhojeet Pramanik, Shashank Mujumdar, and Hima Patel. Towards a multi-modal, multi-task learning based pre-training framework for document representation learning. *arXiv preprint arXiv:2009.14457*, 2020. 3

[33] Ray Smith, Daria Antonova, and Dar-Shyang Lee. Adapting the tesseract open source ocr engine for multilingual ocr. In *Proceedings of the International Workshop on Multilingual OCR*, 2009. 3

[34] Bin Wang, Zhuangcheng Gu, Guang Liang, Chao Xu, Bo Zhang, Botian Shi, and Conghui He. Unimernet: A universal network for real-world mathematical expression recognition, 2024. 3, 4

[35] Bin Wang, Fan Wu, Linke Ouyang, Zhuangcheng Gu, Rui Zhang, Renqiu Xia, Bo Zhang, and Conghui He. Cdm: A reliable metric for fair and accurate formula recognition evaluation. *arXiv:2409.03643*, 2024. 3, 6

[36] Bin Wang, Chao Xu, Xiaomeng Zhao, Linke Ouyang, Fan Wu, Zhiyuan Zhao, Rui Xu, Kaiwen Liu, Yuan Qu, Fukai Shang, Bo Zhang, Liqun Wei, Zhihao Sui, Wei Li, Botian Shi, Yu Qiao, Dahua Lin, and Conghui He. Mineru: An open-source solution for precise document content extraction. *arXiv:2409.18839*, 2024. 1, 3, 7

[37] Pengfei Wang, Chengquan Zhang, Fei Qi, Shanshan Liu, Xiaoqiang Zhang, Pengyuan Lyu, Junyu Han, Jingtuo Liu, Errui Ding, and Guangming Shi. Pgnet: Real-time arbitrarily-shaped text spotting with point gathering network. In *Proceedings of the AAAI Conference on Artificial Intelligence*, pages 2782–2790, 2021. 3

[38] Peng Wang, Shuai Bai, Sinan Tan, Shijie Wang, Zhihao Fan, Jinze Bai, Keqin Chen, Xuejing Liu, Jialin Wang, Wenbin Ge, et al. Qwen2-vl: Enhancing vision-language model's perception of the world at any resolution. *arXiv preprint arXiv:2409.12191*, 2024. 3, 7

[39] Haoran Wei, Chenglong Liu, Jinyue Chen, Jia Wang, Lingyu Kong, Yanming Xu, Zheng Ge, Liang Zhao, Jianjian Sun, Yuang Peng, et al. General ocr theory: Towards ocr-2.0 via a unified end-to-end model. *arXiv:2409.01704*, 2024. 1, 3, 7

[40] Haoran Wei, Lingyu Kong, Jinyue Chen, Liang Zhao, Zheng Ge, Jinrong Yang, Jianjian Sun, Chunrui Han, and Xiangyu Zhang. Vary: Scaling up the vision vocabulary for large vision-language model. In *European Conference on Computer Vision*, pages 408–424. Springer, 2025. 1, 3

[41] Renqiu Xia, Song Mao, Xiangchao Yan, Hongbin Zhou, Bo Zhang, Haoyang Peng, Jiahao Pi, Daocheng Fu, Wenjie Wu, Hancheng Ye, et al. Docgenome: An open large-scale scientific document benchmark for training and testing multi-modal large language models. *arXiv preprint arXiv:2406.11633*, 2024. 1

[42] Renqiu Xia, Bo Zhang, Hancheng Ye, Xiangchao Yan, Qi Liu, Hongbin Zhou, Zijun Chen, Min Dou, Botian Shi, Junchi Yan, et al. Chartx & chartvlm: A versatile benchmark and foundation model for complicated chart reasoning. *arXiv preprint arXiv:2402.12185*, 2024. 1

[43] Zhong Xu, Jianbin Tang, and Antonio Jimeno Yepes. Publaynet: largest dataset ever for document layout analysis. In *2019 International conference on document analysis and recognition*, pages 1015–1022, 2019. 3

[44] Jianshu Zhang, Jun Du, and Lirong Dai. Multi-scale attention with dense encoder for handwritten mathematical expression recognition. In *2018 24th international conference on pattern recognition (ICPR)*, pages 2245–2250. IEEE, 2018. 3

[45] Qintong Zhang, Victor Shea-Jay Huang, Bin Wang, Junyuan Zhang, Zhengren Wang, Hao Liang, Shawn Wang, Matthieu Lin, Wentao Zhang, and Conghui He. Document parsing unveiled: Techniques, challenges, and prospects for structured information extraction. *arXiv preprint arXiv:2410.21169*, 2024. 1

[46] Zhiyuan Zhao, Hengrui Kang, Bin Wang, and Conghui He. Doclayout-yolo: Enhancing document layout analysis through diverse synthetic data and global-to-local adaptive perception, 2024. 3

[47] Xu Zhong, Elaheh ShafieiBavani, and Antonio Jimeno Yepes. Image-based table recognition: data, model, and evaluation. In *European conference on computer vision*, pages 564–580, 2020. 3

[48] Hongbin Zhou, Xiangchao Yan, and Bo Zhang. Structeqtable-deploy: A high-efficiency open-source toolkit for table-to-latex transformation. https://github.com/UniModal4Reasoning/StructEqTable-Deploy, 2024. 8

OmniDocBench: Benchmarking Diverse PDF Document Parsing with Comprehensive Annotations

Supplementary Material

I. More End-to-End Evaluation Results

Table S1 presents the evaluation results of End2End Tables grouped by Table Attributes. As it shows, most of the models perform better in English Tables rather than Chinese ones. Most models perform relatively poorly with Full Frame and No Frame tables. The accuracy of most models is affected by special conditions. Merged cells and formulas mainly test the breadth of data the model can recognize, while colored backgrounds and table rotation test their robustness. The results show that table rotation significantly impacts the accuracy of all models. Pipeline Tools perform well on more challenging tables, but colored backgrounds can affect recognition accuracy. Several Vision Language Models (VLMs) tend to perform worse on tables with merged cells, but colored backgrounds do not significantly impact table recognition accuracy.

Table S2 shows the evaluation results of End2End Text blocks grouped by Text Attributes. Almost all models have lower recognition accuracy in Chinese compared to English. Some models, such as MinerU and Marker, experience a further decrease in accuracy when recognizing mixed Chinese and English content. Complex background colors significantly affect the recognition accuracy of pipeline tools, but they have little impact on VLMs.

II. Dataset Statistics and Visualization

OmniDocBench contains 981 pages, including 9 types of PDF pages, 4 types of layouts, and 3 types of languages. Some pages also include special conditions, such as watermarks. Table S3 and Figure S1 show the number of pages with each page attribute. Figures S3 to S6 are examples of PDF pages with different PDF types, Layout Types, and Special Issues.

Table S6 and Figure S2 show all annotation categories included in OmniDocBench. All of them are annotated by bounding boxes. There are 15 types of block-level annotations and 4 types of span-level annotations, with span-level annotations nested within the block-level ones. In addition, there are 3 types of annotations marked as page interference information (No.20-22), whose bounding boxes are used to mask the specific regions of the PDF pages to avoid affecting the evaluation results. The recognition annotations are also provided for each annotation category except for Figures. Formulas is written in LaTeX format and Table is annotated in both HTML and LaTeX formats. Others are annotated in plain text.

Furthermore, the Text Attributes are also annotated for each block-level category that contains text. There are 3 types of Text Attributes that might influent OCR accuracy: Language, Text Background Color, and Text Rotation. Table S5 shows the statistics of annotations with specific text attributes. There are 23,010 block-level annotations are labeled with text attributes.

Tables are also annotated with Table Attributes. There are 6 types of Table Attributes that might influent the Table Recognition accuracy: Language, Table Frame Type, Merge Cell, Colorful Background, Contain Formula, and Rotation. Table S5 shows the numbers of annotations with specific table attributes. Figures S7 and S8 are the examples of Tables with different Frames and Special Issues.

III. Model Results Visualization

Figures S9 to S17 show the examples of Good model outputs and Bad model outputs of Document Parsing among different PDF types. As it shown, different models exhibit varying performance across different PDF types. For example, MinerU detects all handwritten notes as figures, resulting in very low recognition accuracy in Notes. Marker and InternVL2 experience missed detections, leading to lower scores. InternVL2 and Qwen2-VL, in specific PDF types (such as slides or financial reports), tend to merge multi-column text.

Figures S18 to S20 show the examples of Good model outputs and Bad model outputs under special issues of the PDF pages. It shows that Marker tends to generate typos when the PDF pages are fuzzy scanned or with watermarks, while GOT-OCR fails to recognize content on pages with colored backgrounds. MinerU performs well under special situations, while Mathpix occasionally generates typos.

Figures S21 to S24 show examples of Good model outputs and Bad model outputs for PDF pages with different layouts. MinerU has a low reading order score for single-column layouts primarily because most notes are single-column, and MinerU performs poorly in recognizing Notes, leading to a low reading order score accordingly. InternVL2 scores high in Single-Column layouts but scores poorly on Double-Column and Three-Column layouts. It is mainly due to frequent missed content recognition and errors in reading order judgment in multi-column layouts pages. MinerU's reading order and recognition accuracy decrease with complex layouts, primarily because it incorrectly merges multiple columns during recognition.

Figures S27 and S28 show the model's recognition ability under special issues of text. In text recognition with

Model Type	Model	Language			Table Frame Type				Special Situation			
		EN	*ZH*	*Mixed*	*Full*	*Omission*	*Three*	*Zero*	*Merge Cell*(+/-)	*Formula*(+/-)	*Colorful*(+/-)	*Rotate*(+/-)
Pipeline Tools	MinerU	75.7	59.9	**79.6**	60.0	72.8	**70.1**	**60.4**	64.1/66.0	66.7/65.0	59.8/68.1	2.9/66.4
	Marker	52.5	43.0	44.2	41.8	55.3	47.1	52.4	43.8/47.0	42.9/46.6	44.3/46.7	6.3/46.6
	Mathpix	**76.1**	**64.3**	71.9	68.3	**79.3**	67.0	25.8	**71.2**/66.4	**69.8**/67.6	60.5/71.8	20.7/68.8
Expert Vision Models	GOT-OCR	51.9	47.0	49.4	46.2	49.3	51.6	47.2	46.5/49.7	46.4/49.1	40.2/52.7	0.0/49.4
	Nougat	36.5	0.4	0.0	6.3	3.6	22.2	0.0	15.1/9.1	21.2/8.9	2.8/15.3	0.0/11.4
Vision Language Models	GPT4o	71.8	58.8	57.9	63.3	69.5	61.9	31.8	57.5/65.5	61.6/62.9	62.0/63.0	14.5/63.5
	Qwen2-VL	57.4	62.9	72.7	**70.7**	64.1	48.3	57.6	49.4/68.2	48.5/64.7	**63.5**/60.7	**41.6**/61.9
	InterVL2	61.5	59.3	65.9	59.7	66.5	58.7	56.2	49.6/65.9	54.4/61.6	59.4/60.6	7.3/61.1

Table S1. End-to-End Table TEDS Result grouped by Table Attributes

Model Type	Model	Language			Text background		
		EN	*ZH*	*Mixed*	*White*	*Single*	*Multi*
Pipeline Tools	MinerU	**0.123**	**0.206**	0.742	0.163	**0.147**	0.513
	Marker	0.267	0.389	0.499	0.339	0.389	0.497
	Mathpix	0.173	0.774	0.538	0.675	0.554	0.570
Expert Vision Models	GOT-OCR	0.251	0.763	0.266	0.669	0.595	0.440
	Nougat	0.587	0.991	0.983	0.874	0.935	0.972
Vision Language Models	GPT4o	0.170	0.647	0.322	0.536	0.423	0.406
	Qwen2-VL	0.337	0.575	0.310	0.537	0.400	0.233
	InternVL2	0.418	0.606	**0.251**	0.589	0.366	**0.221**

Table S2. End-to-End Text Normalized Edit Distance results grouped by Text Attributes. "Mixed" represents a mixture of Chinese and English, "Single" and "Multi" represent single color and multi color.

complex background colors, Marker may produce errors or miss content, whereas Qwen2-VL still performs well. Most models fail to recognize text when it is rotated 270 degrees. Some vision language models generate hallucinated information based on the content they can recognize.

Figures S29 to S32 show the examples of good and bad model results for tables with different attributes. For three-line tables, RapidTable demonstrates a good performance with accurate structure recognition, while PaddleOCR shows limitations by missing the last column in its outputs. Interestingly, in tables without frames, PaddleOCR performs well with accurate table predictions, while Qwen2-VL-7B exhibits errors in the last two columns. This indicates that the presence or absence of table frames can significantly impact different models' performance in different ways. Rotated tables prove to be particularly challenging, with most models, including GOT-OCR, failing to recognize the table structure. However, StructEqTable shows promising results by correctly identifying most of the table content, though with a few detail errors. For tables containing formula, Qwen2-VL-7B shows more accurate table structure recognition compared to InternVL2-8B.

IV. Model Settings

For pipeline tools such as MinerU, Marker, and Mathpix, default settings are used for evaluation. Specifically, MinerU with Version 0.9.3[5] is employed. For Marker, Version 0.2.17[6] is evaluated. For Nougat, we utilize its 0.1.0-base model (350M). For GOT-OCR, we employ its format OCR mode to output structured data. For general VLMs, we used the GPT4o, Qwen2-VL-72B, and InternVL2-Llama3-76B by setting the *do_sample=False* to ensure the reproducibility.

Category	Attribute Name	Count
PDF Type	Book	104
	PPT2PDF	133
	Research Report	81
	Colorful Textbook	96
	Exam Paper	114
	Magazine	97
	Academic Literature	129
	Notes	116
	Newspaper	111
Layout Type	Single Column	477
	Double Column	126
	Three Column	45
	One&More Mixed	120
	Complex Layout	213
Language	English	290
	Simplified Chinese	612
	Mixed	79
Special Issues	Fuzzy Scan	28
	Watermark	65
	Colorful Background	246

Table S3. The Page Attributes Statistics of OmniDocBench.

[5] https://github.com/opendatalab/MinerU/releases/tag/magic_pdf-0.9.3-released

[6] https://github.com/VikParuchuri/marker/releases/tag/v0.2.17

Attribute Category	Category Name	Count
Language	English	5857
	Simplified Chinese	16073
	EN&CH Mixed	1080
Text Background	White	19465
	Single-Colored	1116
	Multi-Colored	2429
Text Rotate	Normal	22865
	Rotate90	14
	Rotate270	58
	Horizontal	421

Table S4. Text Attributes Statistics of OmniDocBench.

Attribute Category	Category Name	Count
Language	English	128
	Simplified Chinese	285
	EN&CH Mixed	15
Table Frame Type	Full Frame	205
	Omission Line	62
	Three Line	147
	No Frame	14
Special Issues	Merge Cell	150
	Colorful Background	142
	Contain Formula	81
	Rotate	7

Table S5. Table Attributes Statistics of OmniDocBench.

No.	Category Name	Explaination	Total
1	Title	Include main titles, chapter titles, etc.	2972
2	Text Block	Text paragraphs, which are usually separated by double line breaks in Markdown.	15979
3	Figure	Including images, visual charts, etc.	989
4	Figure Caption	Typically starts with 'Figure' followed by a number, or just descriptive language below the figure.	651
5	Figure Footnotes	Descriptive language, apart from the figure caption, usually starts with an asterisk (*).	133
6	Table	Content organized in table form usually includes borders or a clear table structure.	428
7	Table Caption	Typically starts with 'Table' followed by a number, or just descriptive language above the Table.	299
8	Table Footnotes	Descriptive language, apart from the table caption, usually starts with an asterisk (*).	132
9	Header	Information located at the top of a PDF page or in the sidebar, separate from the main content, typically includes chapter names and other details.	1271
10	Footer	Information located at the bottom of a PDF page, separate from the main content, typically includes the publisher's name and other details.	541
11	Page Number	It is usually represented by numbers, which may be located at the top, in the sidebar, or at the bottom of the page.	669
12	Page Footnote	It provides further explanation of the footnotes marked within the page content. For example, information about the authors' affiliations.	92
13	Code Block	In Markdown, a code block is typically defined using triple backticks (‘‘‘).	13
14	Code Block Caption	Descriptive language above the Code Block.	/
15	Reference	Typically found only in academic literature.	260
16	Text Span	Span-Level text box, which is the plain text content can be directly written in Markdown format.	73143
17	Equation Inline	Formulas that need to be represented using LaTeX format and embedded within the text.	4009
18	Equation Ignore	Some formulas that can be displayed correctly without using LaTeX formatting, such as *15 kg*.	3685
19	Footnote Mark	Typically embedded within the text as superscripts or subscripts, and their numbering usually corresponds to page footnotes.	357
20	Other Abandoned Categories	(Masked) Some uncategorizable, irrelevant page information, such as small icons, etc.	538
21	Masked Text Block	(Masked) Some difficult-to-recognize information that disrupts text flow, such as pinyin annotations above Chinese characters.	34
22	Organic Chemical Formula	(Masked) Organic chemistry formulas, which are difficult to write using Markdown and are easily recognized as Figures.	24

Table S6. Annotation Explanations and Statistics.

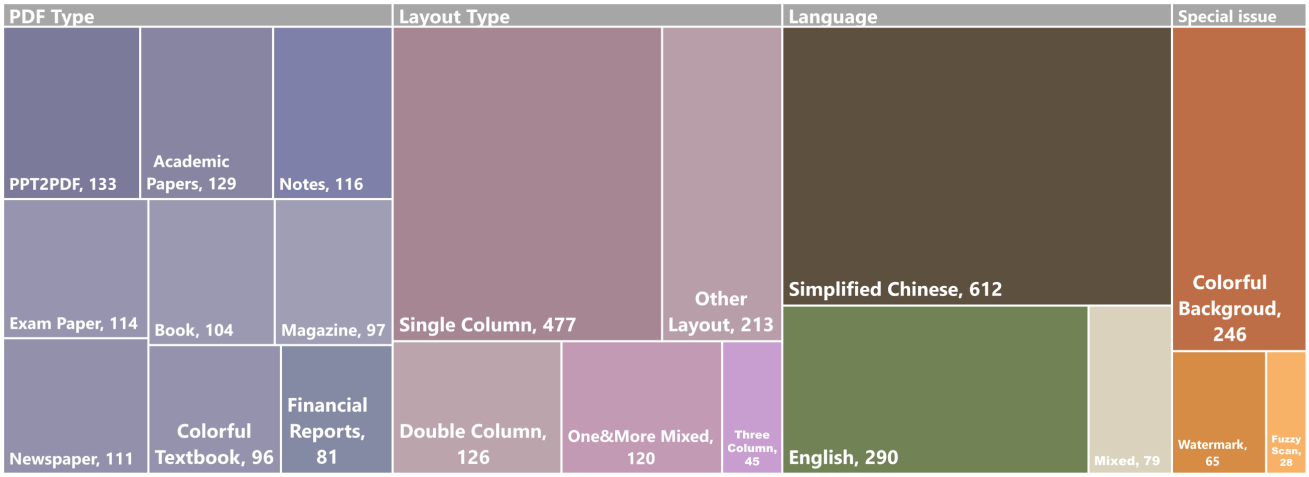

Figure S1. The Data Proportion of Pages for each Attribute in OmniDocBench.

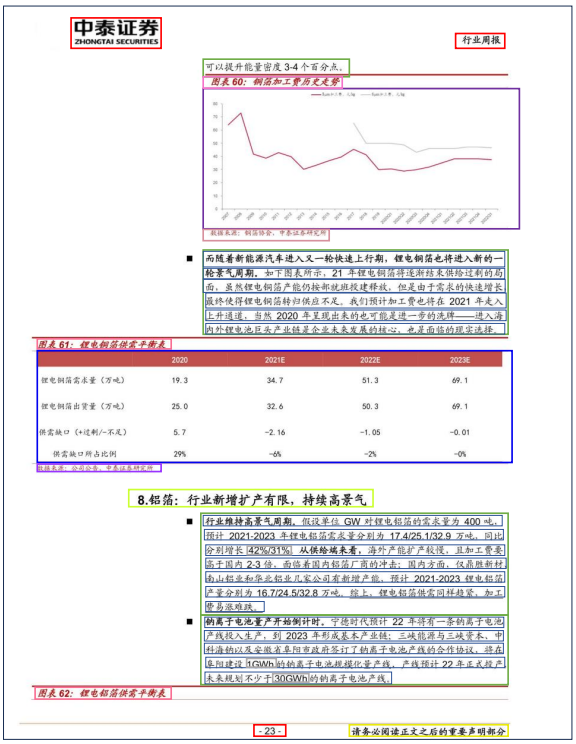

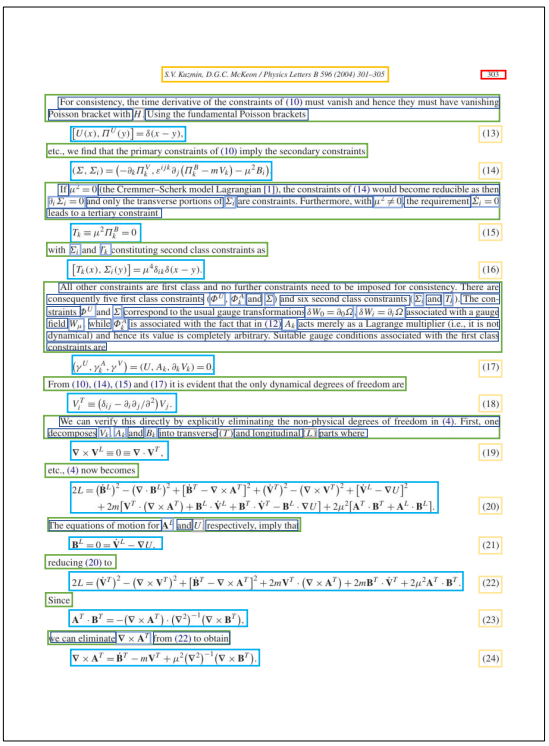

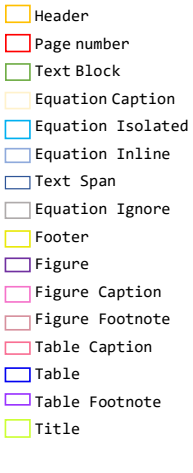

Figure S2. The Visualization of vary Annotations in OmniDocBench.

Figure S3. The Examples of Academic Papers, Books, Textbooks, Notes, and Magazines in OmniDocBench.

Financial Reports

Newspapers

Exam Papers

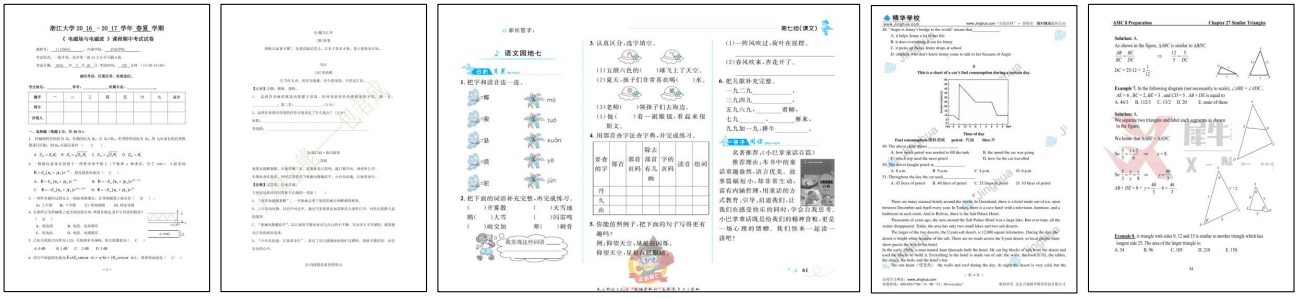

Slides

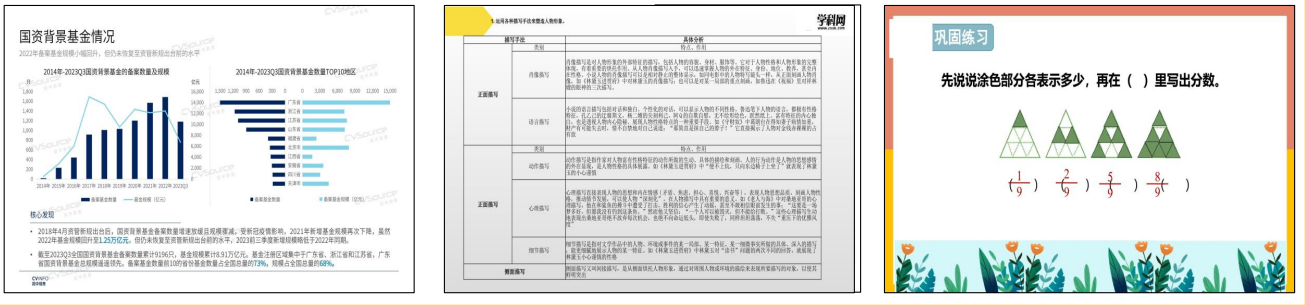

Figure S4. The Examples of Finacial Reports, Newspapers, Example Papers, and Slides in OmniDocBench.

Double Column

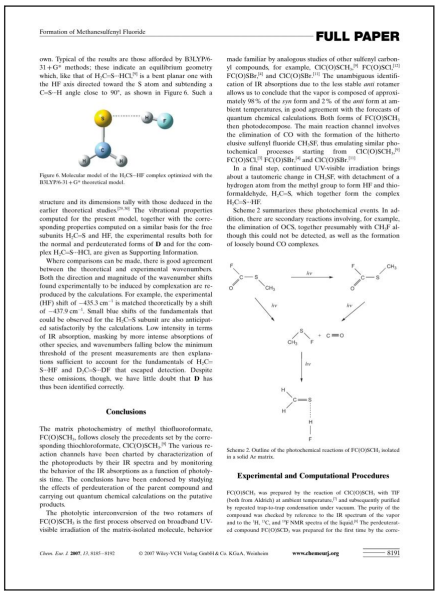

Formation of Methanesulfenyl Fluoride

FULL PAPER

own. Typical of the results are those afforded by B3LYP/6-31+G* methods; these indicate an equilibrium geometry which, like that of $H_2C{=}S{\cdots}HCl$,[16] is a bent planar one with the HF axis directed toward the S atom and subtending a C–S–H angle close to 90°, as shown in Figure 6. Such a

Figure 6. Molecular model of the $H_2CS{\cdots}HF$ complex optimized with the B3LYP/6-31+G* theoretical model.

structure and its dimensions tally with those deduced in the earlier theoretical studies.[16–18] The vibrational properties computed for the present model, together with the corresponding properties computed on a similar basis for the free subunits $H_2C{=}S$ and HF, the experimental results both for the normal and perdeuterated forms of **D** and for the complex $H_2C{=}S{\cdots}HCl$, are given as Supporting Information.

Where comparisons can be made, there is good agreement between the theoretical and experimental wavenumbers. Both the direction and magnitude of the wavenumber shifts found experimentally to be induced by complexation are reproduced by the calculations. For example, the experimental (HF) shift of $-435.3\ cm^{-1}$ is matched theoretically by a shift of $-437.9\ cm^{-1}$. Small blue shifts of the fundamentals that could be observed for the $H_2C{=}S$ subunit are also anticipated satisfactorily by the calculations. Low intensity in terms of IR absorption, masking by more intense absorptions of other species, and wavenumbers falling below the minimum threshold of the present measurements are then explanations sufficient to account for the fundamentals of $H_2C{=}S{\cdots}HF$ and $D_2C{=}S{\cdots}DF$ that escaped detection. Despite these omissions, though, we have little doubt that **D** has thus been identified correctly.

Conclusions

The matrix photochemistry of methyl thiofluoroformate, FC(O)SCH$_3$, follows closely the precedents set by the corresponding thiochloroformate, ClC(O)SCH$_3$.[8] The various reaction channels have been charted by characterization of the photoproducts by their IR spectra and by monitoring the behavior of the IR absorptions as a function of photolysis time. The conclusions have been endorsed by studying the effects of perdeuteration of the parent compound and carrying out quantum chemical calculations on the putative products.

The photolytic interconversion of the two rotamers of FC(O)SCH$_3$ is the first process observed on broadband UV-visible irradiation of the matrix-isolated molecule, behavior made familiar by analogous studies of other sulfenyl carbonyl compounds, for example, ClC(O)SCH$_3$,[8] FC(O)SCl,[22] FC(O)SBr,[20] and ClC(O)SBr.[22] The unambiguous identification of IR absorptions due to the less stable *anti* rotamer allows us to conclude that the vapor is composed of approximately 98% of the *syn* form and 2% of the *anti* form at ambient temperatures, in good agreement with the forecasts of quantum chemical calculations. Both forms of FC(O)SCH$_3$ then photodecompose. The main reaction channel involves the elimination of CO with the formation of the hitherto elusive sulfenyl fluoride CH$_3$SF, thus emulating similar photochemical processes starting from ClC(O)SCH$_3$,[8] FC(O)SCl,[22] FC(O)SBr,[20] and ClC(O)SBr.[22]

In a final step, continued UV-visible irradiation brings about a tautomeric change in CH$_3$SF, with detachment of a hydrogen atom from the methyl group to form HF and thioformaldehyde, $H_2C{=}S$, which together form the complex $H_2C{=}S{\cdots}HF$.

Scheme 2 summarizes these photochemical events. In addition, there are secondary reactions involving, for example, the elimination of OCS, together presumably with CH$_4$ although this could not be detected, as well as the formation of loosely bound CO complexes.

Scheme 2. Outline of the photochemical reactions of FC(O)SCH$_3$ isolated in a solid Ar matrix.

Experimental and Computational Procedures

FC(O)SCH$_3$ was prepared by the reaction of ClC(O)SCH$_3$ with TlF (both from Aldrich) at ambient temperatures,[5] and subsequently purified by repeated trap-to-trap condensation under vacuum. The purity of the compound was checked by reference to the IR spectrum of the vapor and to the ^{1}H, ^{13}C, and ^{19}F NMR spectra of the liquid.[5] The perdeuterated compound FC(O)SCD$_3$ was prepared for the first time by the corresponding

Chem. Eur. J. **2007**, *13*, 8185–8192 © 2007 Wiley-VCH Verlag GmbH & Co. KGaA, Weinheim www.chemeurj.org 8191

Three Column

Federal Register / Vol. 81, No. 194 / Thursday, October 6, 2016 / Rules and Regulations 69427

listing is appropriate; we require evidence that these stressors are operative threats to the species and its habitat, either singly or in combination, to the point that the species meets the definition of an endangered or a threatened species under the Act.

In making our 12-month findings, we considered and evaluated the best available scientific and commercial information regarding the past, present, and future stressors and threats. We reviewed the petition, information available in our files, and other available published and unpublished information. This evaluation may include information from recognized experts; Federal, State, and tribal governments; academic institutions; foreign governments; private entities, and other members of the public.

Arizona Treefrog, Huachuca-Canelo Population (*Hyla wrightorum*)

Previous Federal Actions

In our annual candidate notice of review (CNOR) published on December 6, 2007 (72 FR 69034), we recognized the Huachuca-Canelo population of the Arizona treefrog as a candidate for listing as a distinct population segment (DPS). Subsequently, we published similar findings in our CNORs on December 10, 2008 (73 FR 75176), November 9, 2009 (74 FR 57804), November 10, 2010 (75 FR 69222), October 26, 2011 (76 FR 66370), November 21, 2012 (77 FR 69994), November 22, 2013 (78 FR 70104), December 5, 2014 (79 FR 72450), and December 24, 2015 (80 FR 80584). In 2007, the Huachuca-Canelo population of the Arizona treefrog was assigned a listing priority number (LPN) of 3, reflecting the taxonomic identity of the listable entity as a subspecies/population with threats that we considered to be imminent and high in magnitude. The LPN numbers range from 1 to 11, with 1 being the highest priority.

Background

The Arizona treefrog (*Hyla wrightorum*) is a small (4.6 centimeters (cm) [1.8 inches (in)]) green frog with a dark eyestripe that extends past the shoulder onto the side of the body, and sometimes to the groin area. It occurs in Madrean oak woodland and savannah, pine-oak woodland, mixed conifer forest, and Plains grasslands at elevations of approximately 1,525 to 2,590 meters (m) (5,000 to 8,500 feet (ft)), and requires ponds for successful reproduction.

The Arizona treefrog is known to occur within Arizona, New Mexico, and Mexico. In Arizona and New Mexico, the Arizona treefrog occurs along the Mogollon Rim (central Arizona and western New Mexico), in the Huachuca Mountains and Canelo Hills area (a disjunct mountain range on the Arizona/Sonora, Mexico border), and farther south in Mexico (in the Sierra Madre Occidental and sky island mountain ranges). We refer to these three areas as the Mogollon Rim, Huachuca-Canelo, and Mexico populations.

Within the Huachuca-Canelo population, historical information has documented Arizona treefrogs from three general localities at Rancho Los Fresnos, Sonora, Mexico, and from 13 to 15 verified localities in the Huachuca Mountains and Canelo Hills, Arizona. The Huachuca-Canelo population of Arizona treefrog has continued to persist in Arizona sky island mountain range and Plains grassland habitats, and the treefrog has recently been found in new locations within grasslands and ciénegas (a swamp or marsh, especially one formed and fed by springs) in Arizona. These new localities in varied habitats indicate that the Arizona treefrogs may be less selective in choosing breeding habitat than previously thought. In addition, the species likely occurs in other wet canyons with suitable breeding habitat in the Huachuca Mountains, and perhaps in ciénegas in the vicinity of Rancho Los Fresnos.

The Huachuca-Canelo DPS of the Arizona treefrog was originally defined based on the historical locations. However, recently the Service has received information on Arizona treefrog locations nearby, but outside of, the DPS area. This new information, along with many new location detections in the Huachuca Mountains and Canelo Hills, indicates that the Arizona treefrog is not only more numerous, but is much more widespread than we knew when the Service made this Arizona treefrog a candidate species as a DPS. There are now approximately more than 30 known localities in Arizona in the Huachuca Mountains and Canelo Hills, and the Arizona treefrog also occurs in areas outside of the DPS boundary, but within the vicinity of the Huachuca Mountains and Canelo Hills.

Summary of Status Review

Based on new information and review of previously referenced studies, we find that the Huachuca-Canelo population of the Arizona treefrog does not meet the requirements of the Service's Policy Regarding the Recognition of Distinct Vertebrate Population Segments (DPS Policy) published in the **Federal Register** on February 7, 1996 (61 FR 4722). The DPS Policy sets forth three elements for the Service to consider in determining whether a vertebrate population is a DPS that warrants listing. Whether the population is discrete and whether the population is significant. If the population is determined to be both discrete and significant, then the DPS Policy requires the Service to evaluate the conservation status of the population to determine whether the population meets the Act's definition of an "endangered species" or of a "threatened species."

On the basis of the best available scientific and commercial information, and in accordance with our DPS Policy, we conclude that the Huachuca-Canelo population of the Arizona treefrog is discrete but it is not significant (i.e., it is not biologically or ecologically important) to the taxon as a whole. Regarding discreteness, we have reviewed the best available scientific and commercial information and the evidence relative to potential differences in physical, behavioral, morphological, and genetic attributes. We conclude that the Huachuca-Canelo population of the Arizona treefrog is discrete based on its geographical separation from the other two populations on the Mogollon Rim and in Mexico.

Regarding significance, we considered the four classes of information listed in the DPS Policy as possible considerations in making a determination, as well as all other information that might be relevant to making this determination for the Huachuca-Canelo population. The Huachuca-Canelo population of the Arizona treefrog does not appear to exhibit any direct or indirect habitat adaptation or behavioral advantage that would indicate that their persistence in the Huachuca Mountains and Canelo Hills area is biologically or ecologically important to the taxon as a whole. Moreover, we considered the other three considerations that the DPS Policy sets out for evaluating significance, and none of them provides evidence that the Huachuca-Canelo population is significant to the Arizona treefrog as a whole: (1) Loss of the Huachuca-Canelo population would not result in a significant gap in the range; (2) the Huachuca-Canelo population does not represent the only surviving natural occurrence of the Arizona treefrog; and (3) the Huachuca-Canelo population's genetic characteristics do not differ markedly from those of other Arizona treefrog populations.

Complex Layout

2011年3月5日 星期一 5

种植业导刊

【导读】

2011年种植业8大着力点

高产创建 **标准园创建** **节本增效** **统防统治** **市场监管** **防灾减灾**

场子设在村边低洼处一块地里，四面土坡都是看台。几张桌子一字排开当主席台，手动探照灯（一位老乡专门负责的一只大灯）一打，高音喇叭响起来："喂，老乡们，咱村的老虎大开始啦，没吃完饭的快点，抓紧点啦！"一阵催促，一番叮咛，乡音乡味乡亲，土得掉渣，香得可心。

终于开始了，一阵激情四射的起火当头，欢声雷动。高音喇叭里主持人老乡不紧不慢地介绍，场子里壮汉们步调一致地装火，点火，放！一拨又一拨冲天而起的烟火，变换着色彩、姿态和声响，沸腾了宁静的夜空。从没见过这样的烟火阵势，真真五花八门，匪夷所思。各种火伤情长着眼睛长着腿，机灵滴溜，一会儿这样弯曲，一会儿那样继续，一会儿一条横线，一会儿遍地开花。你听听名字吧，什么张飞蹬鼓、火烧战船，金盏玉台盘，拖白莲，星星草，伞火，老虎火，葡萄火，锅子火，老样火，七节火，起火，平火，喷花，宫花……据说光锅子火火请上就有90多种。最感人是伞火，最壮观是老虎火，最气奶奶磅是老样火。

Fuzzy Scan

86

讨论与思考

在《物理 I》的开篇中，我们曾问，假如有一种完全没有摩擦的"理想热机"，它的效率能达到 100%吗？现在，你是否有所领悟？

本节开始提出的设想为什么无法实现？

科学家正在研究一种新技术，利用海洋中不同深度的温度差驱动热机。这为什么是可行的？

卡诺（S. Carnot，1796—1832），法国物理学家，工程师，毕业于巴黎综合工科学校，1824 年提出了关于热机的卡诺循环的十调定理。

开尔文表述

1851 年，英国物理学家威廉·汤姆生（即开尔文勋爵）从热机的工作特点出发，总结出热力学第二定律的另一种表述：不可能从单一热源吸收热量并把它全部用来做功，而不引起其他变化。这种表述称为开尔文表述。

当能量转化与守恒定律对"第一类永动机"做出"不可能制成"的判决后，历史上有许多人转而将思维定势于另一种从单一热源吸热，并把所吸热量都用于对外全部用来对外做功的机器，也就是说，一种效率达到 100%的热机。这种机器称为"第二类永动机"。"第二类永动机"并不违背能量转化与守恒定律，但被标热力学第一定律的开尔文表述，同样可以被出判决："第二类永动机"也是不可能制成的。再过此是热力学第二定律的又一种表述。

案例分析

案例 夏季夏日，闷位同学在允满凉意的空调室内，就空调机的工作过程是否遵循热力学第二定律的问题发生了争论。

一位同学说：空调机工作时，不断地把热量从室内传到室外，耶从低温物体传到高温物体，可见它并不遵循热力学第二定律。

另一位同学说：热力学第一定律是热力学系统的普遍规律，空调机的工作过程不可能违反它。

同人各执一词，都无法使对方信服。请你对他们的论点作出评价。

分析 空调机和电冰箱都是制冷机，它们的工作原理基本相同。为了便于分析，我们以电冰箱为研究对象，认识它的基本结构

66

Watermark

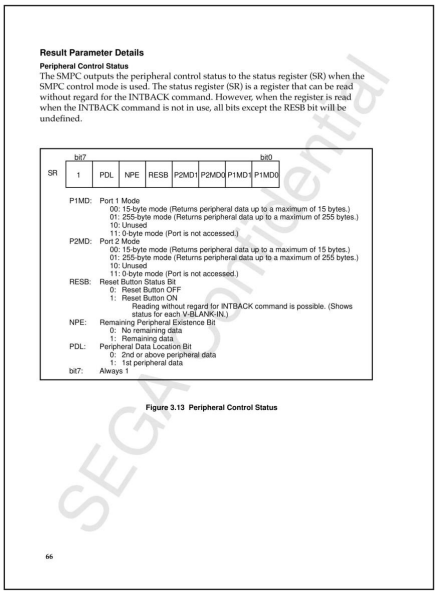

Result Parameter Details

Peripheral Control Status

The SMPC outputs the peripheral control status to the status register (SR) when the SMPC control mode is used. The status register (SR) is a register that can be read without regard for the INTBACK command. However, when the register is read when the INTBACK command is not in use, all bits except the RESB bit will be undefined.

	bit7						bit0
SR	1	PDL	NPE	RESB	P2MD1	P2MD0	P1MD1	P1MD0

P1MD: Port 1 Mode
00: 15-byte mode (Returns peripheral data up to a maximum of 15 bytes.)
01: 255-byte mode (Returns peripheral data up to a maximum of 255 bytes.)
10: Unused
11: 0-byte mode (Port is not accessed.)

P2MD: Port 2 Mode
00: 15-byte mode (Returns peripheral data up to a maximum of 15 bytes.)
01: 255-byte mode (Returns peripheral data up to a maximum of 255 bytes.)
10: Unused
11: 0-byte mode (Port is not accessed.)

RESB: Reset Button Status Bit
0: Reset Button OFF
1: Reset Button ON
Reading without regard for INTBACK command is possible. (Shows status for each V-BLANK-IN.)

NPE: Remaining Peripheral Existence Bit
0: No remaining data
1: Remaining data

PDL: Peripheral Data Location Bit
0: 2nd or above peripheral data
1: 1st peripheral data

bit7: Always 1

Figure 3.13 Peripheral Control Status

SEGA Confidential

Colorful Background

这个你看火神的木架子，四面都有玻璃，这一笔销秀的打书，不知是出自谁人之手。

Figure S6. The Examples of PDF pages under Special Issues in OmniDocBench.

Full Frame

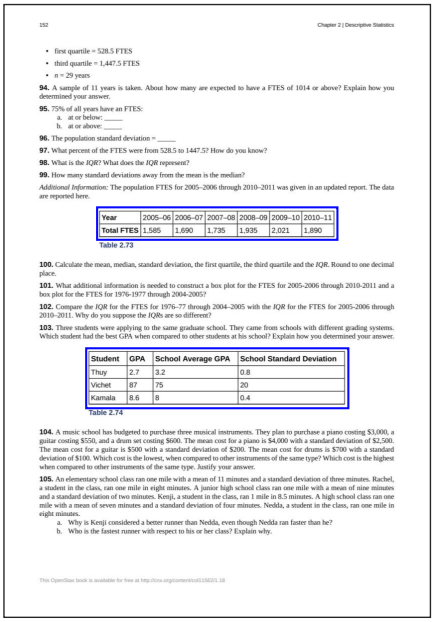

152 Chapter 2 | Descriptive Statistics

- first quartile = 528.5 FTES
- third quartile = 1,447.5 FTES
- n = 29 years

94. A sample of 11 years is taken. About how many are expected to have a FTES of 1014 or above? Explain how you determined your answer.

95. 75% of all years have an FTES:
a. at or below: _____
b. at or above: _____

96. The population standard deviation = _____

97. What percent of the FTES were from 528.5 to 1447.5? How do you know?

98. What is the *IQR*? What does the *IQR* represent?

99. How many standard deviations away from the mean is the median?

Additional Information: The population FTES for 2005–2006 through 2010–2011 was given in an updated report. The data are reported here.

Year	2005–06	2006–07	2007–08	2008–09	2009–10	2010–11
Total FTES	1,585	1,690	1,735	1,935	2,021	1,890

Table 2.73

100. Calculate the mean, median, standard deviation, the first quartile, the third quartile and the *IQR*. Round to one decimal place.

101. What additional information is needed to construct a box plot for the FTES for 2005-2006 through 2010-2011 and a box plot for the FTES for 1976-1977 through 2004-2005?

102. Compare the *IQR* for the FTES for 1976–77 through 2004–2005 with the *IQR* for the FTES for 2005-2006 through 2010–2011. Why do you suppose the *IQR*s are so different?

103. Three students were applying to the same graduate school. They came from schools with different grading systems. Which student had the best GPA when compared to other students at his school? Explain how you determined your answer.

Student	GPA	School Average GPA	School Standard Deviation
Thuy	2.7	3.2	0.8
Vichet	87	75	20
Kamala	8.6	8	0.4

Table 2.74

104. A music school has budgeted to purchase three musical instruments. They plan to purchase a piano costing $3,000, a guitar costing $550, and a drum set costing $600. The mean cost for a piano is $4,000 with a standard deviation of $2,500. The mean cost for a guitar is $500 with a standard deviation of $200. The mean cost for drums is $700 with a standard deviation of $100. Which cost is the lowest, when compared to other instruments of the same type? Which cost is the highest when compared to other instruments of the same type. Justify your answer.

105. An elementary school class ran one mile with a mean of 11 minutes and a standard deviation of three minutes. Rachel, a student in the class, ran one mile in eight minutes. A junior high school class ran one mile with a mean of nine minutes and a standard deviation of two minutes. Kenji, a student in the class, ran 1 mile in 8.5 minutes. A high school class ran one mile with a mean of seven minutes and a standard deviation of four minutes. Nedda, a student in the class, ran one mile in eight minutes.
a. Why is Kenji considered a better runner than Nedda, even though Nedda ran faster than he?
b. Who is the fastest runner with respect to his or her class? Explain why.

This OpenStax book is available for free at http://cnx.org/content/col11562/1.18

Omission Line

352 IEEE TRANSACTIONS ON NANOTECHNOLOGY, VOL. 6, NO. 3, MAY 2007

A New Capacitorless 1T DRAM Cell: Surrounding Gate MOSFET With Vertical Channel (SGVC Cell)

Hoon Jeong, Ki-Whan Song, Il Han Park, Tae-Hun Kim, Yeun Seung Lee, Seong-Goo Kim, Jun Seo, Kyoungyong Cho, Kangyoon Lee, Hyungcheol Shin, *Member, IEEE*, Jong Duk Lee, *Member, IEEE*, and Byung-Gook Park, *Member, IEEE*

***Abstract*—We propose a surrounding gate MOSFET with vertical channel (SGVC cell) as a 1T DRAM cell. To confirm the memory operation of the SGVC cell, we simulated its memory effect and fabricated the highly scalable SGVC cell. According to simulation and measurement results, the SGVC cell can operate as a 1T DRAM having a sufficiently large sensing margin. Also, due to its vertical channel structure and common source architecture, it can readily be made into a 4F^2 cell array.**

***Index Terms*—Memory effect, 1T DRAM cell, sensing margin, surrounding gate, vertical channel.**

TABLE I
SGVC CELL SIMULATION PARAMETERS

	Program (1/0) (Impact Ionization)	Read
Gate Voltage	1 V	1 V
Drain Voltage	1 V (-1 V)	0.1 V
Source Voltage	0 V	0 V

L_{gate} length=0.1 um t_{ox} (gate oxide)=50 Å
t_{Si} (Pillar Diameter)= 60 nm
$N_{s/d}$ (source/drain region doping)=10^{20} cm^{-3} (graded doping)
N_{body} (body doping) =10^{18} cm^{-3}
$t_{overlap}$ =10 nm

I. Introduction

TO OVERCOME the scalability issues and process complexity of 1-transistor/1-capacitor DRAM cell, capacitorless 1-transistor (1T) DRAM cells have been recently proposed and investigated [1]. The mainstream 1T DRAM cell is a floating body transistor cell (FBC) which consists of a MOSFET with its body floating electrically. The FBC is realized by a MOSFET formed on partially depleted silicon-on-insulator (PD-SOI). When excess holes exist in the floating body, the cell state can be defined as "1" (decreased V_{th}). On the other hand, when excess holes are swept out of the floating body through forward bias on the body–drain junction, the cell state can be defined as "0" (increased V_{th}). By measuring the drain current difference between "1" and "0" states of the cell, we can sense whether the holes are accumulated in the floating body. Because the floating body is used as the storage node, the FBC has no complicated storage capacitor. Therefore, the FBC has a simple process and can have a cell area below 4F^2 [2], [3].

In this work, we propose a surrounding gate MOSFET with vertical channel (SGVC cell) as a 1T DRAM cell. Unlike other 1T DRAM cells which are integrated on SOI substrates, the SGVC cell can be more cost effective since it can be fabricated on bulk Si substrates. Also, there is no need for the source contact and line due to the common source structure, which makes 4F^2 structure possible and ultimately leads to superior scalability. The memory operation has been investigated by simulation. Also, we have successfully fabricated a highly scalable SGVC cell and the memory effect is measured for the first time.

Manuscript received June 18, 2006; revised December 9, 2006. This work was presented at the 2006 IEEE Silicon Nanoelectronics Workshop. The review of this paper was arranged by Associate Editor T. Hiramoto.

H. Jeong, I. H. Park, T.-H. Kim, Y. S. Lee, H. Shin, J. D. Lee and B.-G. Park are with the School of Electrical Engineering, Seoul National University, Seoul 151-742, Korea (e-mail: ghhtt@snuver.com).
K.-W. Song is with the ATD Team, Semiconductor R&D Division, Samsung Electronics Co. Ltd., Yongin 449-711, Korea.
S.-G. Kim and K. Lee are with the Technology Development Team, Semiconductor R&D Division, Samsung Electronics Co. Ltd., Yongin 449-711, Korea.
J. Seo and K. Cho is with the Process Development Team, Semiconductor R&D Division, Samsung Electronics Co. Ltd., Yongin 449-711, Korea

Color versions of one or more of the figures in this paper are available online at http://ieeexplore.ieee.org.
Digital Object Identifier 10.1109/TNANO.2007.893575

II. Simulation Results

Fig. 1 schematically shows the operation principle of an SGVC cell [4]. It can be noted that it has a floating body where holes are accumulated for memory effects. To verify memory cell operation, 2-D device simulation was performed. We used ATLAS as a simulator. Excess holes are generated by impact ionization in this simulation. Simulated parameters are listed in Table I. The difference in the body potential of each state and the $I_D - V_G$ characteristics were extracted first, in order to show the accumulation of holes in the body of the SGVC cell. Fig. 2 shows a comparison of the hole potential between "1" state and reference state ($V_{gate} = 0$, $V_{source} = 0$, $V_{drain} = 0$). In the case of state "1," through impact ionization in the high field region near the drain, excess holes are injected into the body and then the body potential increases. Fig. 3 shows $I_D - V_G$ characteristics of the SGVC cell. The drain current of "1" state is larger than that of "0" state. This is due to the increase of the body potential when holes are accumulated into the body through writing operation, hence lowering the threshold voltage, which in turn increases the drain current. Subsequently, the drain current as a function of time was extracted to show

1536-125X/$25.00 © 2007 IEEE

Tree Line

中国物联网平台行业竞争格局——物联网平台主要玩家类型

物联网平台行业企业数量不断增加，企业凭自身核心优势，以不同的目的和角度入局，按照企业属性将进入物联网平台产业的主要玩家划分为五种类型。

企业类型	目的	模式和特点	优势	典型企业
云服务提供商	• 以物联网为抓手带动上层应用服务业绩增长	• 目前多以提供底层行算资源，很快以应用使能平台为主	• 在互联网领域中积累了丰富的技术、商业、生态优势积极 • 底层IaaS能力突出，具有技术能力服务	阿里云、腾讯云、百度云、亚马逊AWS IoT等
通信领域厂商	• 获得流量业务收入，维略布局物联网，积攒新增市场机遇	• 多以连接管理、应用使能为平台主要功能服务为主	• 在连接管理平台具有绝对优势，具有全球通用连接能力	电信运营商、通信设备厂商、中国电信天翼物联、联中国移动OneNet、中国联通物联网平台、华为云IoT等
软件系统服务商	• 解决传统开发效率的问题，优化产品服务	• 以应用开发平台为主要服务内容为主	• 围绕软件设计、生产、管理、运维等服务具备丰富的行业软件开发及服务经验	紫光云、广联达筑联等
垂直领域传统厂商	• 利用自身对行业的理解与经验，打造垂直型平台，实现传统企业的转型升级	• 垂直专业领域的物联网平台	• 深刻的行业理解和行业技术，对行业有深度应用，拥有行业数据和客户资源	西门子、工业富联、美的M-Smart等企业
初创企业	• 看好物联网未来的发展潜能	• 目前初级根多初创型平台企业多以OpenStack为核心的开源开发	• 拥有与底层细分行业相关的软件、硬件经验 • 服务故事和选择型平台厂商等以触及的细分领域，形成强互竞争	涂鸦智能、云智易、初智云、支云物联等

来源：公开资料整理，头部研究院

No Frame

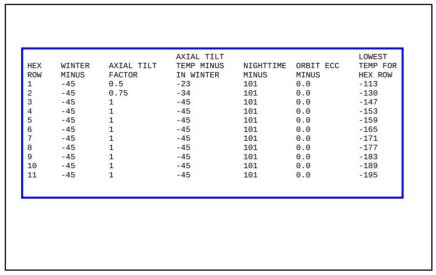

HEX ROW	WINTER MINUS	AXIAL TILT FACTOR	AXIAL TILT TEMP MINUS IN WINTER	NIGHTTIME MINUS	ORBIT ECC MINUS	LOWEST TEMP FOR HEX ROW
1	-45	0.5	-23	101	0.0	-113
2	-45	0.75	-34	101	0.0	-130
3	-45	1	-45	101	0.0	-147
4	-45	1	-45	101	0.0	-153
5	-45	1	-45	101	0.0	-159
6	-45	1	-45	101	0.0	-165
7	-45	1	-45	101	0.0	-171
8	-45	1	-45	101	0.0	-177
9	-45	1	-45	101	0.0	-183
10	-45	1	-45	101	0.0	-189
11	-45	1	-45	101	0.0	-195

Figure S7. The Examples of Tables with different Frame in OmniDocBench.

Table Rotate

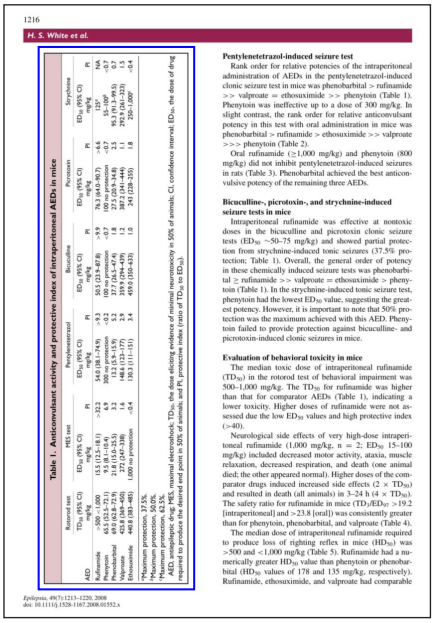

1216 H. S. White et al.

Table I. Anticonvulsant activity and protective index of intraperitoneal AEDs in mice

AED	Rotorod test TD$_{50}$ (CI) mg/kg	PI	MES test ED$_{50}$ (CI) mg/kg	PI	Pentylenetetrazol ED$_{50}$ (CI) mg/kg	PI	Bicuculline ED$_{50}$ (CI) mg/kg	PI	Strychnine ED$_{50}$ (CI) mg/kg	PI
Rufinamide	>500 (–1,000)	>19.2	145 (128–164)	>9.3	76.3 (64.0–90.7)	>6.6	165 (123–87.8)	>9.9	120*	N/A
Phenobarbital	69.0 (62.8–72.9)	2.3	32.4 (28.5–36.5)	2.1	15.2 (13.0–17.5)	2.0	37.5 (30.0–46.9)	2.2	51.2 (47.1–55.3)	0.7
Phenytoin	65.0 (62.8–72.9)	1.2	13.2 (5.9–15.9)	5.2	95.3 (91.5–99.5)	2.5	377 (26.5–47.4)	1.8	27.5 (20.9–34.8)	2.4
Valproate	318 (310–326)	1.2	270 (247–295)	1.2	311 (279–347)	1.0	320 (277–370)	1.2	272 (253–293)	1.1
Ethosuximide	>400 (381–418)	<0.4	>1,000 no protection	<0.4	>1,000 no protection	<0.4	>1,000 no protection	<0.4	243 (228–259)	1.8

*Maximum protection, 37.5%.
†Maximum protection, 62.5%.
‡Maximum protection, 50%.
AED, antiepileptic drug; MES, maximal electroshock; TD$_{50}$, the dose eliciting evidence of minimal neurotoxicity in 50% of animals; CI, confidence interval; ED$_{50}$, the dose of drug required to produce the desired end point in 50% of animals; and PI, protective index (ratio of TD$_{50}$ to ED$_{50}$).

Epilepsia, 49(7):1213–1220, 2008
doi: 10.1111/j.1528-1167.2008.01552.x

Pentylenetetrazol-induced seizure test

Rank order for relative potencies of the intraperitoneal administration of AEDs in the pentylenetetrazol-induced clonic seizure test in mice was phenobarbital > rufinamide >> valproate = ethosuximide >> phenytoin (Table 1). Phenytoin was ineffective up to a dose of 300 mg/kg. In slight contrast, the rank order for relative anticonvulsant potency in this test with oral administration in mice was phenobarbital > rufinamide > ethosuximide >> valproate >>> phenytoin (Table 2).

Oral rufinamide (≥1,000 mg/kg) and phenytoin (800 mg/kg) did not inhibit pentylenetetrazol-induced seizures in rats (Table 3). Phenobarbital achieved the best anticonvulsive potency of the remaining three AEDs.

Bicuculline-, picrotoxin-, and strychnine-induced seizure tests in mice

Intraperitoneal rufinamide was effective at nontoxic doses in the bicuculline and picrotoxin clonic seizure tests (ED_{50} ~50–75 mg/kg) and showed partial protection from strychnine-induced tonic seizures (37.5% protection; Table 1). Overall, the general order of potency in these chemically induced seizure tests was phenobarbital ≥ rufinamide >> valproate = ethosuximide > phenytoin (Table 1). In the strychnine-induced tonic seizure test, phenytoin had the lowest ED_{50} value, suggesting the greatest potency. However, it is important to note that 50% protection was the maximum achieved with this AED. Phenytoin failed to provide protection against bicuculline- and picrotoxin-induced clonic seizures in mice.

Evaluation of behavioral toxicity in mice

The median toxic dose of intraperitoneal rufinamide (TD_{50}) in the rotorod test of behavioral impairment was 500–1,000 mg/kg. The TD_{50} for rufinamide was higher than that for comparator AEDs (Table 1), indicating a lower toxicity. Higher doses of rufinamide were not assessed due the low ED_{50} values and high protective index (>40).

Neurological side effects of very high-dose intraperitoneal rufinamide (1,000 mg/kg, n = 2; ED_{50} 15–100 mg/kg) included decreased muscle activity, ataxia, muscle relaxation, decreased respiration, and death (one animal died; the other appeared normal). Higher doses of the comparator drugs induced increased side effects (2 × TD_{50}) and resulted in death (all animals) in 3–24 h (4 × TD_{50}). The safety ratio for rufinamide in mice (TD_{50}/ED_{50}) >19.2 [intraperitoneal] and >23.8 [oral]) was consistently greater than for phenytoin, phenobarbital, and valproate (Table 4).

The median dose of intraperitoneal rufinamide required to produce loss of righting reflex in mice (HD_{50}) was >500 and <1,000 mg/kg (Table 5). Rufinamide had a numerically greater HD_{50} value than phenytoin or phenobarbital (HD_{50} values of 178 and 135 mg/kg, respectively). Rufinamide, ethosuximide, and valproate had comparable

Table contain Formula

第三章 铁 金属材料

素呈+3 价，在进行有关氧化还原反应的计算时，可将 Fe 元素的化合价看作+$\frac{8}{3}$ 价。Fe_3O_4 可以用 FeO · Fe_2O_3 来表示，但 Fe_3O_4 是化合物，是一种纯净物，不能将 Fe_3O_4 看成是由 FeO 和 Fe_2O_3 组成的混合物。

问题 3 金属阳离子被还原一定得到金属单质吗？

不一定，存在多种价态的金属可能从较高价态被还原到较低价态，但仍为化合态，如铁粉与氯化铁溶液的反应：$Fe+2Fe^{3+}=\!=\!=3Fe^{2+}$。

印象笔记

◀四氧化三铁是一种常用的磁性材料，特制的纯净四氧化三铁用来作录音磁带和电讯器材的原材料。煮光打印机的墨粉中也含有四氧化三铁。

应试拓展注意

拓展 1 铁的氧化物和氢氧化物

铁的氧化物比较

名称	氧化亚铁	氧化铁（俗称铁红）	四氧化三铁（俗称磁性氧化铁）
化学式	FeO	Fe_2O_3	Fe_3O_4
颜色、状态	黑色粉末	红棕色粉末	黑色晶体
铁的价态	+2 价	+3 价	+2、+3 价
水溶性	均不溶于水		
与非氧化性酸反应	$FeO+2H^+=\!=\!=Fe^{2+}+H_2O$	$Fe_2O_3+6H^+=\!=\!=2Fe^{3+}+3H_2O$	$Fe_3O_4+8H^+=\!=\!=Fe^{2+}+2Fe^{3+}+4H_2O$
与 H_2、CO、Al 等反应	$FeO+H_2\xrightarrow{\triangle}Fe+H_2O$	$Fe_2O_3+3CO\xrightarrow{高温}2Fe+3CO_2$	$3Fe_3O_4+8Al\xrightarrow{高温}9Fe+4Al_2O_3$

◀放宫红墙（显红色主要是因为含有 Fe_2O_3）

【说明】(1) FeO 不稳定，易被氧化为 Fe_3O_4。

(2) FeO、Fe_3O_4 遇氧化性酸（如 HNO_3）发生氧化还原反应，+2 价的铁均被氧化为+3 价。

(3) FeO、Fe_2O_3 均为碱性氧化物，Fe_3O_4 是复杂的氧化物，不属于碱性氧化物。

铁的磁体比较铁制品与铁制饭手

铁矿石

铁的氢氧化物比较

名称	氢氧化亚铁	氢氧化铁
化学式	$Fe(OH)_2$	$Fe(OH)_3$
颜色、状态	白色固体	红褐色固体
水溶性	不溶	不溶
与酸反应	$Fe(OH)_2+2H^+=\!=\!=Fe^{2+}+2H_2O$	$Fe(OH)_3+3H^+=\!=\!=Fe^{3+}+3H_2O$
稳定性	不稳定，在空气中会迅速由白色变为灰绿色，最后变为红褐色：$4Fe(OH)_2+O_2+2H_2O=\!=\!=4Fe(OH)_3$	常温下稳定，加热分解 $2Fe(OH)_3\xrightarrow{\triangle}Fe_2O_3+3H_2O$
制备	$Fe^{2+}+2OH^-=\!=\!=Fe(OH)_2\downarrow$（必须在非氧化性环境中制备）	$Fe^{3+}+3OH^-=\!=\!=Fe(OH)_3\downarrow$

◀$Fe(OH)_3$ 为白色絮状沉淀，在空气中迅速被氧化，白色→灰绿色→红褐色，此知识点常作为元素存在的检验方法和物质推断的重要突破口。

Table with Colorful Background

2021五一假期全国5A级热门爬山景区预测

同程旅游

- 依据同程交通大数据预测：五一期间南安市泰山风景名胜区、佛祖市云台山风景名胜区、黄山市黄山等5A级爬山景区将迎引较多的游客；
- 提醒自驾前往景区的游客请安全、尤其行驶在盘山路上时，要保持安全车距，外出、山顶温差较大，提醒前往登山的游客带好保暖衣服，避免着凉。

2021年全国5A级热门爬山景区TOP 10 预测

城市	景区
泰安市	泰山风景名胜区
南平市	云台山风景名胜区
黄山市	黄山
舟山市	普陀山风景名胜区
长沙市	五台山风景名胜区
渭南市	华山风景名胜区
衡阳市	罗浮山风景名胜区
台安市	武功山国家级风景名胜区
铜仁市	梵净山风景区
池州市	九华山风景区

数据来源于高德地图和各旅游局

Table with Merge Cell

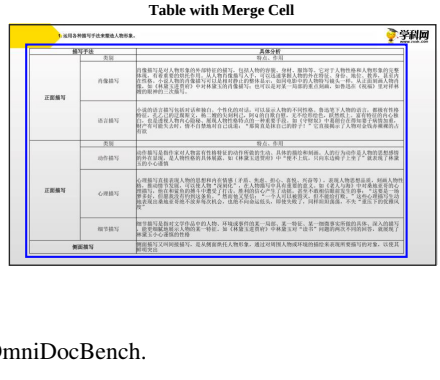

描写手法		具体分析
	类别	简介、作用
正面描写	肖像描写	肖像描写是指对人物的容貌外表等进行描写，如对人物的容貌、神情、姿势等。它对人物性格和人物形象的塑造有着重要的作用。不仅要关注人物的外在特征，还要关注人物的内在精神。在进行肖像描写时，可以运用细致入微的笔触，对人物的外貌特征进行详细的描绘，以展现出人物的个性和内在世界。同时，还要注意肖像描写与人物的性格、情感和故事情节之间的关联，使其成为整个故事不可或缺的一部分。
	语言描写	人物语言描写是指对话和独白的描写，不仅仅是说话，而是通过人物的语言，揭露他们的性格、态度和情感。在人们的日常生活中，我们每天都会与不同的人进行交流，这些交流中的语言不仅仅是简单的对话，更是一种深层次的沟通。通过观察和分析人们的语言，我们可以更好地理解他们的内心世界，从而更好地与他们建立联系。
	其他	动作描写、心理描写、细节描写
正面描写	其他	动作描写是指在叙述人物的言行举止时，对人物的动作进行描写，以展现人物的性格特点和情感状态。在日常生活中，我们每天都会观察到各种各样的人物，他们的动作和行为都反映了他们的内心世界和性格特点。通过对这些动作的描写，我们可以更好地理解人物的行为动机，从而更好地与他们进行交流和互动。
	心理描写	心理描写是指在叙述人物的言行举止时，对人物的心理活动进行描写，以展现人物的内心世界和情感状态。在日常生活中，我们每天都会观察到各种各样的人物，他们的言行举止背后都隐藏着他们的内心世界和情感状态。通过对这些心理活动的描写，我们可以更好地理解人物的行为动机，从而更好地与他们进行交流和互动。
	细节描写	细节描写是指对人物的言行举止进行详细的描写，以展现人物的性格特点和情感状态。在日常生活中，我们每天都会观察到各种各样的人物，他们的言行举止背后都隐藏着他们的内心世界和情感状态。通过对这些细节的描写，我们可以更好地理解人物的行为动机，从而更好地与他们进行交流和互动。
侧面描写		侧面描写是指对人物的言行举止进行详细的描写，以展现人物的性格特点和情感状态。在日常生活中，我们每天都会观察到各种各样的人物，他们的言行举止背后都隐藏着他们的内心世界和情感状态。通过对这些侧面描写的描写，我们可以更好地理解人物的行为动机，从而更好地与他们进行交流和互动。

Figure S8. The Examples of Tables under Special Issues in OmniDocBench.

Academic Papers

usually have partial myelitis and characteristically have asymmetric clinical findings with predominantly sensory symptoms. Spinal MRI lesions usually extend over less than two spinal segments. As in the other subtypes of CIS, abnormal brain MRI results is the most robust factor to predict conversion, followed by the presence of OBs.[7,26,27] Notably, none of our 20 patients with myelitis and normal baseline MRI results has experienced development of a second attack or a new T2 lesion in the 1-year MRI after a mean follow-up of 44 months (data not shown).

CISs classically refer to ON, brainstem syndromes, or spinal cord syndromes. Less common initial episodes suggestive of central nervous system demyelination such as hemispheric or clinically polyregional syndromes have not been specifically studied. In our cohort, only 30 patients (9.4%) had an initial attack different from classical CISs: 12 patients (3.8%) had a polyregional syndrome, 6 had a hemispheric syndrome (1.9%), and 12 (3.8%) had a neurological syndrome of undetermined topography. In our cohort of patients, there are insufficient numbers in this subgroup of patients to draw useful conclusions. A consensus definition of what is multifocal or polyregional needs to be achieved, and a greater number of patients with such characteristics should be studied.

The apparent discrepancy between natural history studies that claimed that ON has a better outcome and the prospective cohort on CISs and clinical trials that do not show differences in outcomes among different topographies may be explained by our observational study, which demonstrates that, overall, patients with ON may have a better outcome because, as a group, they have more chances for normal baseline MRI results than patients with other CISs. Differential diagnosis in patients with subacute visual loss is comprehensible, and other causes that mimic inflammatory-demyelinating ON are difficult to identify. Nevertheless, if a patient with ON has abnormal baseline MRI results, his or her prognosis does not differ from that of other patients with different CISs. MRI at baseline, not CIS topography, appears to be the crucial issue at MS presentation.

References

1. Confavreux C, Vukusic S, Adeleine P. Early clinical predictors and progression of irreversible disability in multiple sclerosis: an amnesic process. Brain 2003;126:770–782.
2. Weinshenker BG, Bass GP, Rice J, et al. The natural history of multiple sclerosis: a geographically based study. 1. Clinical course and disability. Brain 1989;112:133–146.
3. Weinshenker BG. Natural History of Multiple Sclerosis. Ann Neurol 1994;36:S6–S11.
4. Runmarker B, Andersen O. Prognostic factors in multiple sclerosis incidence cohort with twenty-five years of follow-up. Brain 1993;116:117–136.
5. Brex PA, Ciccarelli O, Jonathan L, et al. A longitudinal study of abnormalities on MRI and disability from multiple sclerosis. N Engl J Med 2002;346:158–164.
6. Morrissey SP, Miller DH, Kendall BE, et al. The significance of brain magnetic resonance imaging abnormalities at presentation with clinically isolated syndromes suggestive of multiple sclerosis. A 5-year follow-up study. Brain 1993;116:135–146.
7. O'Riordan JI, Thompson AJ, Kingsley DPE, et al. The prognostic value of brain MRI in clinically isolated syndromes of the CNS: a 10 year follow-up. Brain 1998;121:495–503.
8. Jacobs LD, Beck RW, Simon JH, et al. Intramuscular interferon-beta-1a therapy initiated during a first demyelinating event in multiple sclerosis. N Engl J Med 2000;343:898–904.
9. Comi G, Filippi M, Barkhof F, et al. Effect of early interferon treatment on conversion to definite multiple sclerosis: a randomised study. Lancet 2001;357:1576–1582.
10. Tintoré M, Rovira A, Río J, et al. Optic neuritis brainstem syndromes and myelitis: early conversion to multiple sclerosis. Mol Clin (Barc) 1999;112:693–696.
11. Tintoré M, Rovira A, Río J, et al. New diagnostic criteria for multiple sclerosis: application in first demyelinating episode. Neurology 2003;60:27–30.
12. Frohman EM, Goodin DS, Calabresi PA, et al. The utility of MRI in suspected MS: Report of the therapeutics and technology assessment subcommittee of the American Academy of Neurology. Neurology 2003;61:602–611.
13. McDonald WI, Compston A, Edan G, et al. Recommended diagnostic criteria for multiple sclerosis: guidelines from the international panel on the diagnosis of multiple sclerosis. Ann Neurol 2001;50:121–127.
14. Andersson M, Alvarez-Cermeño J, Bernardi G, et al. Cerebrospinal fluid in the diagnosis of multiple sclerosis: a consensus report. J Neurol Neurosurg Psychiatry 1994;57:897–902.
15. Barkhof F, Filippi M, Miller DH, et al. Comparison of MRI criteria at first presentation to predict conversion to clinically definite multiple sclerosis. Brain 1997;120:2059–2069.
16. Poser CM, Paty DW, Scheinberg L, et al. New diagnostic criteria for multiple sclerosis: guidelines for research protocols. Ann Neurol 1983;13:227–231.
17. Tintoré M, Rovira A, Martínez MJ, et al. Isolated demyelinating syndromes: comparison of different MRI criteria to predict conversion to clinically definite multiple sclerosis. Am J Neuroradiol 2000;21:702–706.
18. Beck RW, Cleary PA, Anderson MM Jr, et al. A randomized, controlled trial of corticosteroids in the treatment of acute optic neuritis. The Optic Neuritis Study Group. N Engl J Med 1992;27:581–588.
19. Río J, Nos C, Rovira A, et al. The development of multiple sclerosis following an isolated episode of optic neuritis. Magnetic resonance study. Mol Clin (Barc) 1997;109:370–372.
20. Rodriguez M, Siva A, Cross SA, et al. Optic neuritis: a population-based study in Olmsted County, Minnesota. Neurology 1995;45:244–250.
21. Miller DH, Ormerod IEC, McDonald WI, et al. The early risk of multiple sclerosis after optic neuritis. J Neurol Neurosurg Psychiatry 1988;51:1569–1571.
22. Soderström M, Ya-Ping J, Hillert J, Link H. Optic neuritis. Prognosis for multiple sclerosis from MRI, CSF and HLA findings. Neurology 1998;50:708–714.
23. Jacobs LD, Kaba SE, Miller CM, et al. Correlation of clinical, MRI and CSF findings in optic neuritis. Ann Neurol 1997;41:392–398.

214 Annals of Neurology Vol 57 No 2 February 2005

Markdown Content (MinerU)

usually have partial myelitis and characteristically have asymmetric clinical findings with predominantly sensory symptoms. ..... , none of our 20 patients with myelitis and normal baseline MRI results has experienced development of a second attack or a new T2 lesion in the 1-year MRI after a mean follow-up of 44 months (data not shown).

CISs classically refer to ON, brainstem syndromes, or spinal cord syndromes. ..... . A consensus definition of what is multifocal or polyregional needs to be achieved, and a greater number of patients with such characteristics should be studied.

The apparent discrepancy between natural history studies that claimed that ON has a better outcome ..... MRI at baseline, not CIS topography, appears to be the crucial issue at MS presentation.

References

1. Confavreux C, Vukusic S, Adeleine P ..... 126:770-782.

2. Weinshenker BG, Bass GP, Rice J, et al. ..... ;112:133-146.

3. Weinshenker BG. Natural History of Multiple ..... .;36:S6-S11.

4. Runmarker B, Andersen O. ..... 1993;116:117-134.

●●●

22. Sodersrom M, Ya-Ping J, Hillet J, Link H. ..... 1998;50:708-714.

23. Jacobs LD, Kaba SE, Miller CM, et al. l .....1997 41: 392-398.

Markdown Content (InternVL2)

---Missing Content---

5. Brex PA, Ciccarelli O, Jonathan L, et al. ..... 2002;346:158-164.

6. Morrissey SP, Miller DH, Kendall BE, et al. ..... 1993;56:5-13.

●●●

22. Sodersrom M, Ya-Ping J, Hillet J, Link H. ..... 1998;50:708-714.

23. Jacobs LD, Kaba SE, Miller CM, et al. l .....1997 41: 392-398.

Figure S9. The Good Model Result and Bad Model Result for Academic Papers.

Book

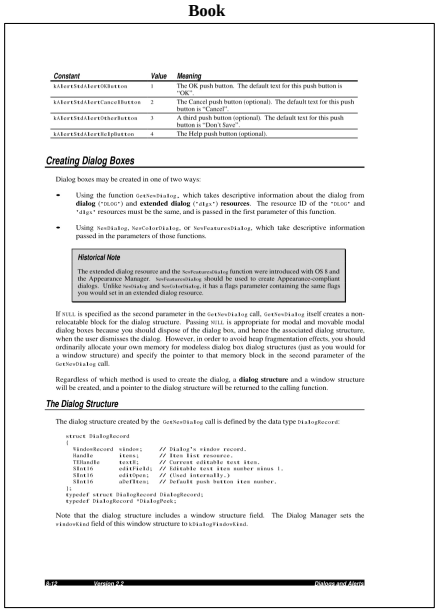

Constant	Value	Meaning
kAlertStdAlertOKButton	1	The OK push button. The default text for this push button is "OK".
kAlertStdAlertCancelButton	2	The Cancel push button (optional). The default text for this push button is "Cancel".
kAlertStdAlertOtherButton	3	A third push button (optional). The default text for this push button is "Don't Save".
kAlertStdAlertHelpButton	4	The Help push button (optional).

Creating Dialog Boxes

Dialog boxes may be created in one of two ways:

- Using the function GetNewDialog, which takes descriptive information about the dialog from **dialog** ('DLOG') and **extended dialog** ('dlgx') **resources**. The resource ID of the 'DLOG' and 'dlgx' resources must be the same, and is passed in the first parameter of this function.
- Using NewDialog, NewColorDialog, or NewFeaturesDialog, which take descriptive information passed in the parameters of those functions.

Historical Note

The extended dialog resource and the NewFeaturesDialog function were introduced with OS 8 and the Appearance Manager. NewFeaturesDialog should be used to create Appearance-compliant dialogs. Unlike NewDialog and NewColorDialog, it has a flags parameter containing the same flags you would set in an extended dialog resource.

If NULL is specified as the second parameter in the GetNewDialog call, GetNewDialog itself creates a nonrelocatable block for the dialog structure. Passing NULL is appropriate for modal and movable modal dialog boxes because you should dispose of the dialog box, and hence the associated dialog structure, when the user dismisses the dialog. However, in order to avoid heap fragmentation effects, you should ordinarily allocate your own memory for modeless dialog box dialog structures (just as you would for a window structure) and specify the pointer to that memory block in the second parameter of the GetNewDialog call.

Regardless of which method is used to create the dialog, a **dialog structure** and a window structure will be created, and a pointer to the dialog structure will be returned to the calling function.

The Dialog Structure

The dialog structure created by the GetNewDialog call is defined by the data type DialogRecord:

```
struct DialogRecord
{
  WindowRecord  window;     // Dialog's window record.
  Handle        items;      // Item list resource.
  TEHandle      textH;      // Current editable text item.
  SInt16        editField;  // Editable text item number minus 1.
  SInt16        editOpen;   // (Used internally.)
  SInt16        aDefItem;   // Default push button item number.
};
typedef struct DialogRecord DialogRecord;
typedef DialogRecord *DialogPeek;
```

Note that the dialog structure includes a window structure field. The Dialog Manager sets the windowKind field of this window structure to kDialogWindowKind.

Markdown Content (Mathpix)

<table border=1><tr> <td>Constant</td> <td>Value</td> <td>Meaning</td> </tr><tr><td>kAlertStdAlertOKButton</td> <td>1</td><td><table><tr><td>The OK push button. The default text for this push button is</td></tr><tr><td>"OK".</td></tr></table>.....

Creating Dialog Boxes Dialog boxes may be created in one of two ways:- Using the function GetNewDialog, which takes descriptive information about the dialog from dialog ($\cdot$ DLOG $\cdot$) and extended dialog ${\cdot \mathrm{d} 1 \mathrm{gx} \cdot}$ resources. ..... - Using NewDialog, NewColorDialog, or NewFeaturesDialog, which take descriptive information passed in the parameters of those functions. .....

Historical Note
The extended dialog resource and the NewFeaturesDialog function were introduced with OS 8 and the Appearance Manager. .....

If NULL is specified as the second parameter in the GetNewDialog call, GetNewDialog itself creates a nonrelocatable block for the dialog structure. ..... Regardless of which method is used to create the dialog, a dialog structure and a window structure will be created, and a pointer to the dialog structure will be returned to the calling function.

The Dialog Structure .....{WindowRecord window; // Dialog's window record. Handle items; // Item list resource. TEHandle textH; // Current editable text item. SInt16 editField; // Editable text item number minus 1. SInt16 editOpen; // (Used internally_) SInt16 aDefItem; // Default push button item number. };..... The Dialog Manager sets the windowKind field of this window structure to kDialogWindowKind.

Markdown Content (Nougat)

---Missing Table ---

Creating Dialog Boxes
Dialog boxes may be created in one of two ways:
* Using the function GetNewDialog, which takes descriptive information about the dialog from **dialog** ("dLog") and **extended dialog** ("dIgx") **resources**. The resource ID of the "dLog" and "dIgx" resources must be the same, and is passed in the first parameter of this function. .....

Historical Note
The extended dialog resource and the NewFeaturesDialog function were introduced with OS 8 and the Appearance Manager. .....

If null is specified as the second parameter in the GetNewDialog call, GetNewDialog itself creates a non-relocatable block for the dialog structure. .....
Regardless of which method is used to create the dialog, a **dialog structure** and a window structure will be created, and a pointer to the dialog structure will be returned to the calling function.

The Dialog Structure .....WindowRecord window; // Dialog's window record. Handle items; // Item list resource. TEhandle textH; // Current editable textit item. SInt16 editField; // Editable textit item number minus 1. SInt16 editOpen; // (Used internally.) SInt16 aberIfen; // Default push button item number.); .....The Dialog Manager sets the windowKind field of this window structure to kDialogWindowKind.

Figure S10. The Good Model Result and Bad Model Result for Books.

Exam Papers

Lessons 1～2　测试卷

时间：90 分钟　　满分：100 分

题号	Ⅰ	Ⅱ	Ⅲ	Ⅳ	Ⅴ	Ⅵ	Ⅶ	Ⅷ	Ⅸ	Ⅹ	总分	等级
得分												

听力部分（30 分）

Ⅰ. 听录音，选出你所听到的单词。（10 分）

( )1. A. must　B. much　C. may
( )2. A. put　B. eat　C. sit
( )3. A. seat　B. street　C. skate
( )4. A. line　B. learn　C. light
( )5. A. too　B. into　C. in

Ⅱ. 听录音，按你所听内容，用数字"1～5"给下列图片排序。（10 分）

( )　( )　( )　( )　( )

Ⅲ. 听录音，选择正确的答语。（10 分）

( )1. A. Good afternoon，Mrs Read.　B. Sorry，she's not in.
( )2. A. I'm having lunch.　B. I'm in the park.
( )3. A. Hello，John!　B. Yes. Here it is.
( )4. A. Yes，we can.　B. You're welcome.
( )5. A. You can sit here.　B. At the sports centre.

47

Markdown Content (Qwen2-VL)

```
# Lessons 1 ~ 2 测试卷
时间:90分钟 满分:100分
<table border=\"1\" >\n <tr>\n rowspan=\"1\"> ..... 总分
</td>\n　　<td colspan=\"1\" rowspan=\"1\">等级</td>\n
</tr>\n</table>

## 听力部分 (30 分)
### I. 听录音,选出你所听到的单词。(10 分)
1. A. must B. much C. may
2. A. put B. eat C. sit
3. A. seat B. street C. skate
4. A. line B. learn C. light
5. A. too B. into C. in

### II. 听录音,按你所听内容,用数字"1 ~ 5"给下列图片排序。(10 分)

![图片1](https://i.imgur.com/1.png)
![图片2](https://i.imgur.com/2.png)
![图片3](https://i.imgur.com/3.png)
![图片4](https://i.imgur.com/4.png)
![图片5](https://i.imgur.com/5.png)

### III. 听录音,选择正确的答语。(10 分)
1. A. Good afternoon, Mrs Read. B. Sorry, she's not in.
2. A. I'm having lunch. B. I'm in the park.
3. A. Hello, John! B. Yes. Here it is.
4. A. Yes, we can. B. You're welcome.
5. A. You can sit here. B. At the sports centre.
---
关注微信公众号"教辅资料站"获取更多学习资料
```

Markdown Content (Mathpix)

```
荣冠新课堂 $\cdot$ 五年级英语（下）．KP

Lessons 1 ~ 2 测试卷
时间：90 分钟
满分：100 分
*NI 茹 出 岗 <table border=1>
<tr> <td>题号</td> <td>I</td> <td>II</td><td>III</td>
<td>IV</td> <td>V</td> <td>VI</td> <td>VII</td>
<td>VIII</td> <td>IX</td> <td>X</td> <td>总分</td>
<td>等级</td> </tr> <tr> <td>得分</td> <td></td>
<td></td> <td></td> <td></td><td></td><td></td><td></td>
<td></td><td></td><td></td><td></td><td></td><td></td><td></td><td><
/td></tr></table>管
```

---Prediction Content Error ---

```
听力部分 (30 分)
I. 听录音,选出你所听到的单词。(10 分)
多 $=$ 离 出 管 尖
( ) B. much B. eat B. street B. learn B. into C. may C. sit C. skate
C. light C. in

II. 听录音, 按你所听内容, 用数字" $\mathbf{1 \sim 5 \text { "给下
列图片排序。（10 分） }}$

III. 听录音, 选择正确的答语。(10 分)
( )1. A. Good afternoon, Mrs Read. B. Sorry, she's not in.
( )2. A. I'm having lunch. B. I'm in the park.
( )3. A. Hello, John! B. Yes. Here it is.
( )4. A. Yes, we can. B. You're welcome.
( )5. A. You can sit here. B. At the sports centre.

关注微信公众号"教辅资料站" 47 获取更多
```

Figure S11. The Good Model Result and Bad Model Result for Exam Papers.

Magazines

第四章　主食类

葱油面

材料成分

主料：香葱 500g，大葱 500g，紫葱头 500g，切面（细）5kg；
辅料：水 300g，油菜 500g，食用油 500g；
调料：酱油 1kg。

总材料图

制作过程

香葱切段，大葱、葱头切丝，油菜切开备用；葱油制作：锅内放油烧至三成热，将香葱、大葱、葱头入锅小火熬制 20 分钟后加酱油、水，开锅 10 分钟盛出；锅中煮面条的同时放一个小油菜，煮熟后浇上葱油、撒上香葱粒即可（原料按 35 碗计算）。

成品图

工艺技巧

面条要细；熬油温度不宜太高。

品质特点

柔韧爽滑，葱香可口。

王广勇　提供

157

Markdown Content (MinerU)

```
# 第四章 主食类

## 葱油面

### 材料成分
- **主料**：香葱 500g，大葱 500g，紫葱头 500g，切面（细）5kg；
- **辅料**：水 300g，油菜 500g，食用油 500g；
- **调料**：酱油 1kg。

### 制作过程
香葱切段，大葱、葱头切丝，油菜切开备用；葱油制作：锅内放油烧至三成热，将香葱、大葱、葱头入锅小火熬制20分钟后加酱油、水，开锅10分钟盛出；锅中煮面条的同时放一个小油菜，煮熟后浇上葱油、撒上香葱粒即可（原料按35碗计算）。

### 工艺技巧
面条要细；熬油温度不宜太高。

### 品质特点
柔韧爽滑，葱香可口。
```

Markdown Content (GPT4o)

```
<div align="center">
  <h2>葱油面</h2>
  <img src="image-url" alt="葱油面图片" width="200">
</div>

### 材料成分
<table><tr><td><b>主料：</b>香葱 500g, 大葱 500g, 紫葱头 500g, 切面（细）5kg;</td><td><img src="image-url" alt="原材料图" width="100"></td></tr> <tr>
<d><b>辅料：</b>水 300g, 油菜 500g, 食用油 500g;</td>
  </tr><tr><td><b>调料：</b>酱油 1kg。
</td></tr></table>
```

--- Prediction Category Error ---

```
### 制作过程
香葱切段，大葱、葱头切丝，油菜切开备用；葱油制作: 锅内放油烧至三成热，将香葱、大葱、葱头入锅小火熬制 20 分钟后加酱油、水，开锅 10 分钟盛出；锅中煮面条的同时放一个小油菜，煮熟后浇上葱油，撒上香葱粒即可（原料按 35 碗计算）。

### 工艺技巧
面条要细；熬油温度不宜太高。

### 品质特点
柔韧爽滑，葱香可口。

<div align="right">
  <b>王广勇 提供</b>
</div> <p align="center">157</p>
```

Figure S12. The Good Model Result and Bad Model Result for Magazines.

Newspapers

Markdown Content (MinerU)

三部门再次公布举报电话严查虚假报道

新华社北京12月31日电为深入推动全国新网战线开展"杜绝虚假报道、培强社会责任 .....

据悉，各省、自治区，直辖市有关部门和单位也将陆续公市举报电话。

国家广电总局举报电话： 010-86093956

新闻出版总署举报电话： 010-65212787

中国记协举报电话：010-58262800

新华社北京12月31日电（记者李志勇1211年北京春运期司农民工团体订票将于1月5日开始：.....

记者从北京市交通委了解到.2011年1月5日至16日.北京农民工春运团体票预订将在北京站和北京西站办理：1月10日至22日，农民工可以到北京站，北京西站和北京北站开设的农民工团体售票专口直接购买农民工团体火车票，.....

●●●

票星12009-2011年回库支持排广的农业机楼产品日票】中营庆2006年国家科学技术进步二等奖票获2005年河南省科学技术进步一等奖 中荣获2008年河南省科学技术进步二等奖十国家标准（GB/T24689：1\~GB/T24689.7-2009）.....

001或85815522传真：（010）85832154广告热线：010）84395085广告经营许可证：京朝工商广字第0055号每份：0.63元月价：16.5元农民日报社印刷厂印

Markdown Content (Mathpix)

4 |时事新闻 2011年1月1日 星期六 业民日赫

河南佳多科工稀有限责任公司致以最崇高敬意，并恭祝新春愉快！* 荣获2008年河南少科学技术进步二等奖* 荣录《河南省重点工业产品达标备案目录》政府招投标优先采购产品

每做 $: 0.63 \bar{\pi}$

---Missing Content---

Figure S13. The Good Model Result and Bad Model Result for Newspaper.

Notes

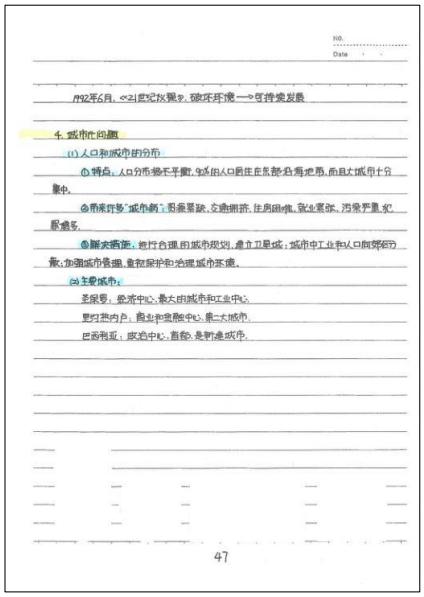

Markdown Content (InternVL2)

```markdown
NO. _____ Date _____

1992年6月，《21世纪议程》破坏环境→可持续发展

4. 城市化问题

(1) 人口和城市的分布

① 特点：人口分布极不平衡，90%的人口居住在东部沿海地带，而且大城市占十分之七。

② 带来许多"城市病"：交通拥堵、住房困难、就业紧张、污染严重、犯罪增多。

③ 解决措施：进行合理的城市规划，建立卫星城；城市中工业和人口向郊区分散；加强城市管理，重视保护和治理城市环境。

(2) 主要城市：

圣保罗：经济中心、最大的城市和工业中心。

里约热内卢：商业和金融中心、第二大城市。

巴西利亚：政治中心、首都，是新建城市。
```

Markdown Content (MinerU)

---Handle Writing Text Missing---

Figure S14. The Good Model Result and Bad Model Result for Handwriting Notes.

Financial Reports

Markdown Content (MinerU)

```
# 广汇能源(600256.SH)单季度业绩再创历史新高，绿色转型迈出步伐

# 核心观点

单季度业绩再创新高。2022年前三季度公司实现营收372.79亿元，同比 $+126.36\%$ ：..... 环比 $+12.14\%$ 在 第三季度主要煤化工装置年度大修影响34天的情况下，公司继续刷新自上市以来单季度业绩新高。

主要产品产销持续增长，海外天然气涨价增厚贸易利润。前三季度公司煤炭销量达到1918.79万吨，同比 $+36.64\%$ ..... ,公司海外天然气贸易显著受益，预计未来几年全球天然气仍然处于紧平衡，因此公司LNG长协贸易套利值得期待。

在建项目进展顺利，绿色能源转型开启新篇章。..... 土建工作基本完成，设备安装完成 $60\%$ 氢能方面，公司投资建设绿电制氢及氢能一体化示范项目，建设6MW风光发电装机，1000Nm2/h电解水制氢等装置，有望在2023年6月建成投产。

●●●

<td><table border="1"><thead><tr><td><b>基础数据</b></td><td><b>买入（维持）..... </td></tr><tr><td>近3个月日均成交额</td><td>1692.78百万元</td></tr></tbody></table></td>

![](images/afd04c030530ca6353f7ce602c5f0b1a093ac2a0e8e5c61bf3142de0ac5b24e0.jpg)

●●●

<td><table border="1"><thead><tr><td><b>盈利预测和财务指标</b></td><td><b> ..... 3.2</td></tr><tr><td>市净率（PB）</td><td>4.94</td><td>3.85</td><td>2.86</td><td>2.04</td><td>1.50</td></tr></tbody></table></td>
```

Markdown Content (Qwen2VL)

国信证券 GUOSEN SECURITIES 证券研究报告 | 2022年10月19日 广汇能源（600256.SH） 单季度业绩再创历史新高，绿色转型迈出步伐 核心观点 公司研究·财报点评 石油石化·炼化及贸易 ..... 2022 年前三季度公司实现营收 372.79 亿元，同比 +126.36%；归母净利润 84.02 亿元，同比+204.37%。其中三季度单季实现营 收 159.58 亿元，环比+33.83%；归母净利润 32.71 亿元，环比+12.14%。在 第二季度主要煤化工装置年度大修影响 34 天的情况下，公司继续刷新自上 市以来单季度业绩新高。 主要产品产销持续增长，海外天然气涨价增厚贸易利润。前三季度公司煤炭 销量达到 1918.79 万吨，同比+36.64%；天然气销量 416.316.16 万方，同比 +24.76%。..... 。 维持 22-24 年公司归母净利润预测为 122/160/204 亿，对应 EPS=1.85/2.44/3.11 元/股，当前股价对应 PE=6.6/5.0/4.0x，维持"买入" 评级。 盈利预测和财务指标 2020 2021 2022E 2023E 2024E 营业收入（百万元） 15,134 24,865 44,837 56,437 68,664 （+/-%） 7.8% 64.3% 80.3% 25.9% 21.7% 净利润（百万元） 1336 5003 12156 16027 20406 （+/-%） -16.3% 274.4% 143.0% 31.8% 27.3% 每股收益（元） 0.20 0.76 1.85 2.44 3.11 EBIT Margin 20.2% 31.5% 40.5% 40.7% 41.8% 净资产收益率（ROE） 8.0% 23.9% 43.1% 40.6% 38.0% 市盈率（PE） 62.1 16.1 6.6 5.0 4.0 EV/EBITDA 26.2 12.5 5.3 4.1 3.2 市净率（PB） 4.94 3.85 2.86 2.04 1.50 资料来源：Wind、国信证券经济研究所预测 注：摊薄每股收益按最新总股本计算 请务必阅读正文之后的免责声明及其项下所有内容

---Merge Multiple Columns to One--

---Missing Table---

---Missing Table---

Figure S15. The Good Model Result and Bad Model Result for Financial Reports.

Slides

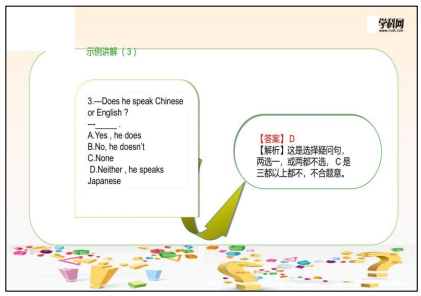

Markdown Content (MinerU)

```
示例讲解 (3)

3.---Does he speak Chinese or English ?
A.Yes , he does
B.No, he doesn't
C.None
D.Neither , he speaks Japanese

# 【答案】

【解析】这是选择疑问句两选一，或两都不选，C是 三都以上都不，不合题意。
```

Markdown Content (Marker)

```
示例讲解(3)

--------Missing Text Content------

![0_image_1.png](0_image_1.png)

![0_image_2.png](0_image_2.png)

![0_image_0.png](0_image_0.png)
```

```
合作探究

改对，包括对文章段落的进一步调整和加工。段落安排是否合理，段与段之间是否衔接，详略安排是否恰当等等，都是修改是应该重点关注的。

![](images/eb64e4894e8beea67242ef779bea7b3900447c5a59ca1cf2aed3f22b7578412d.jpg)
```

```
合作探究 AAAAA

# 0

![0_image_0.png](0_image_0.png)

--------Missing Text Content------
```

Figure S16. The Good Model Result and Bad Model Result for Slides.

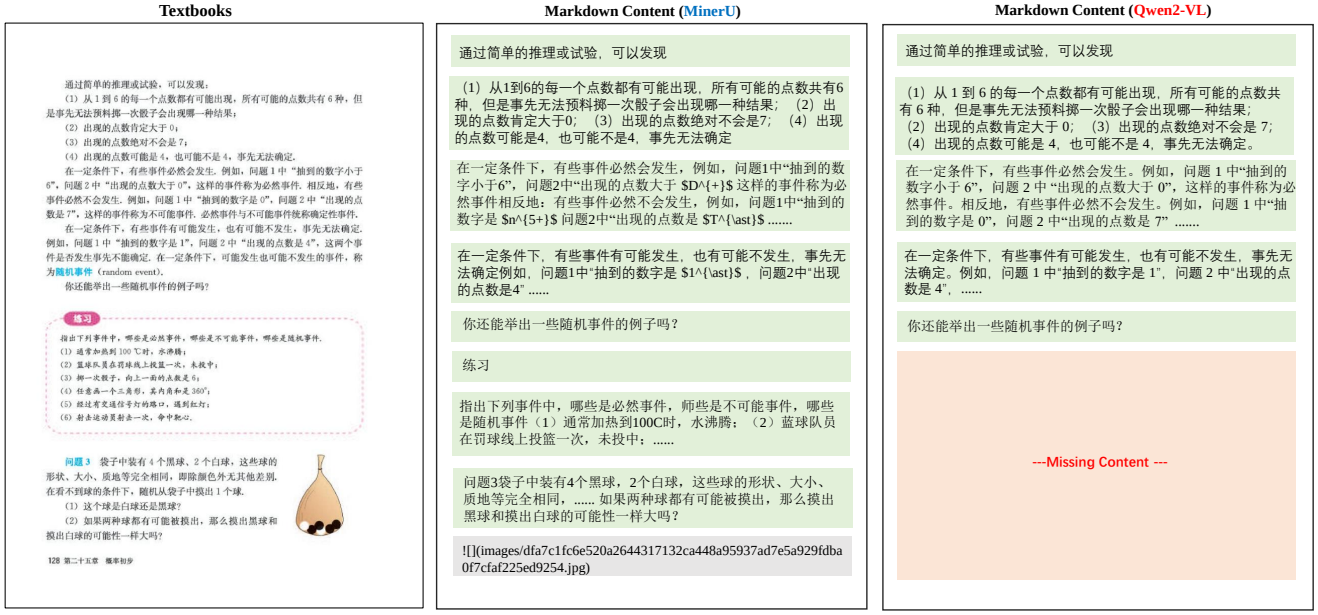

Figure S17. The Good Model Result and Bad Model Result for Textbooks.

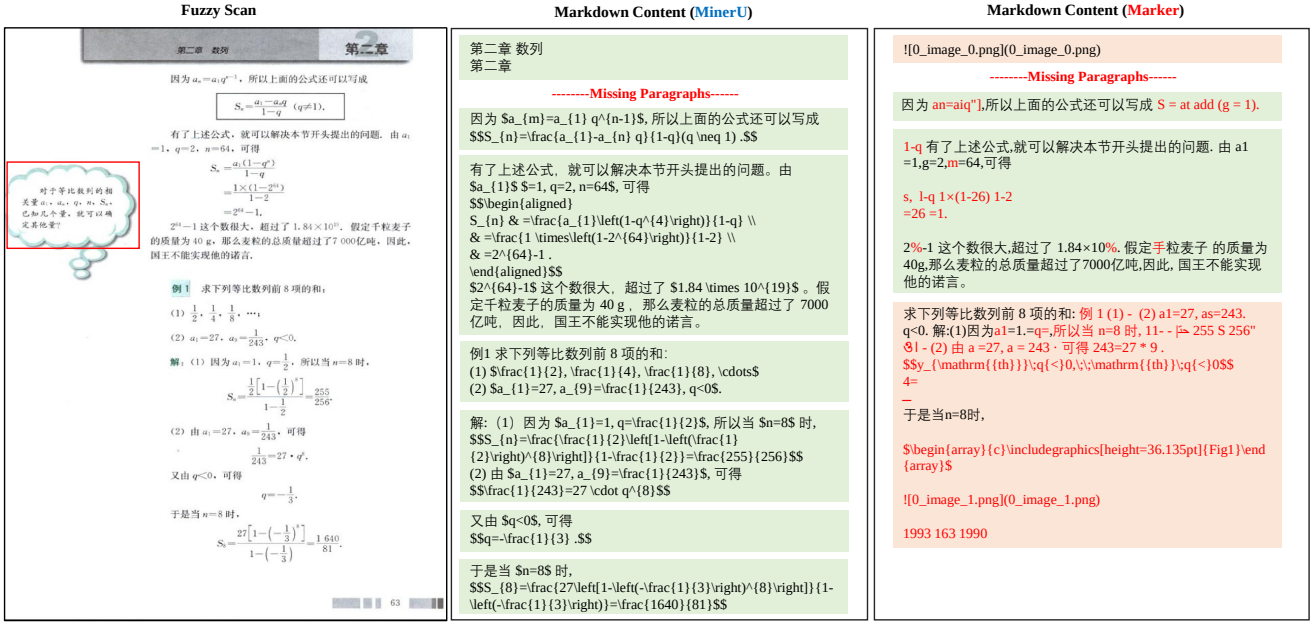

Figure S18. The Good Model Result and Bad Model Result for Fuzzy Scan Pages.

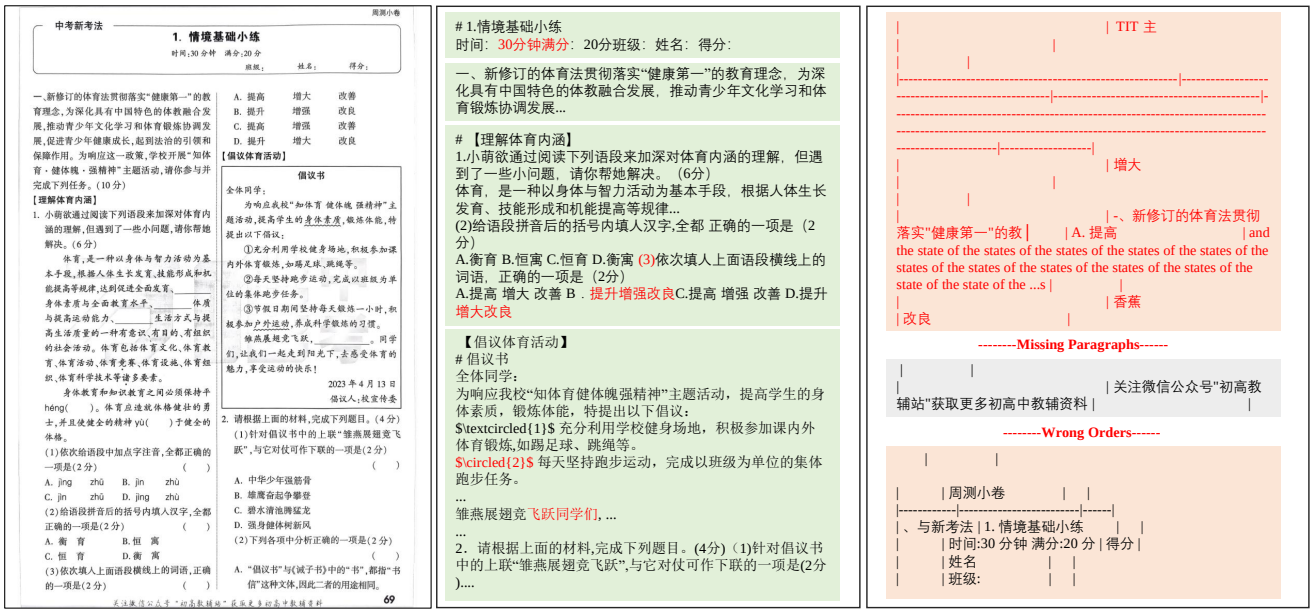

Figure S19. The Good Model Result and Bad Model Result for Pages with Watermark.

Figure S20. The Good Model Result and Bad Model Result for Colorful Background Pages.

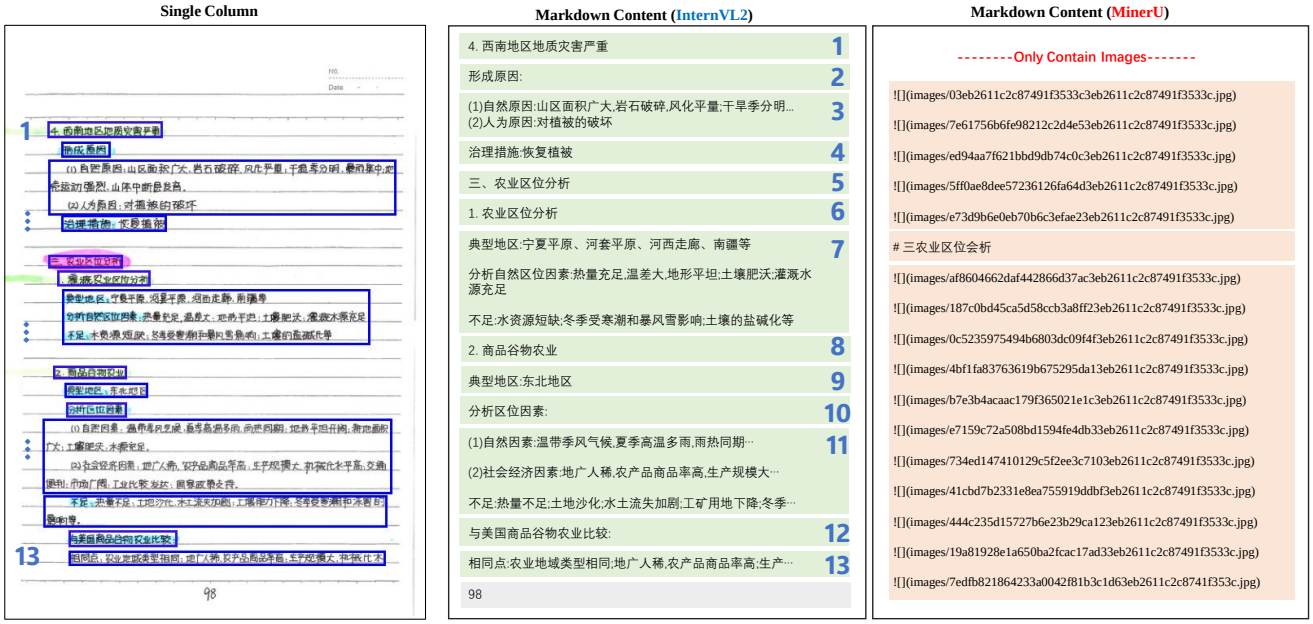

Figure S21. The Good Model Result and Bad Model Result for Single Column Pages.

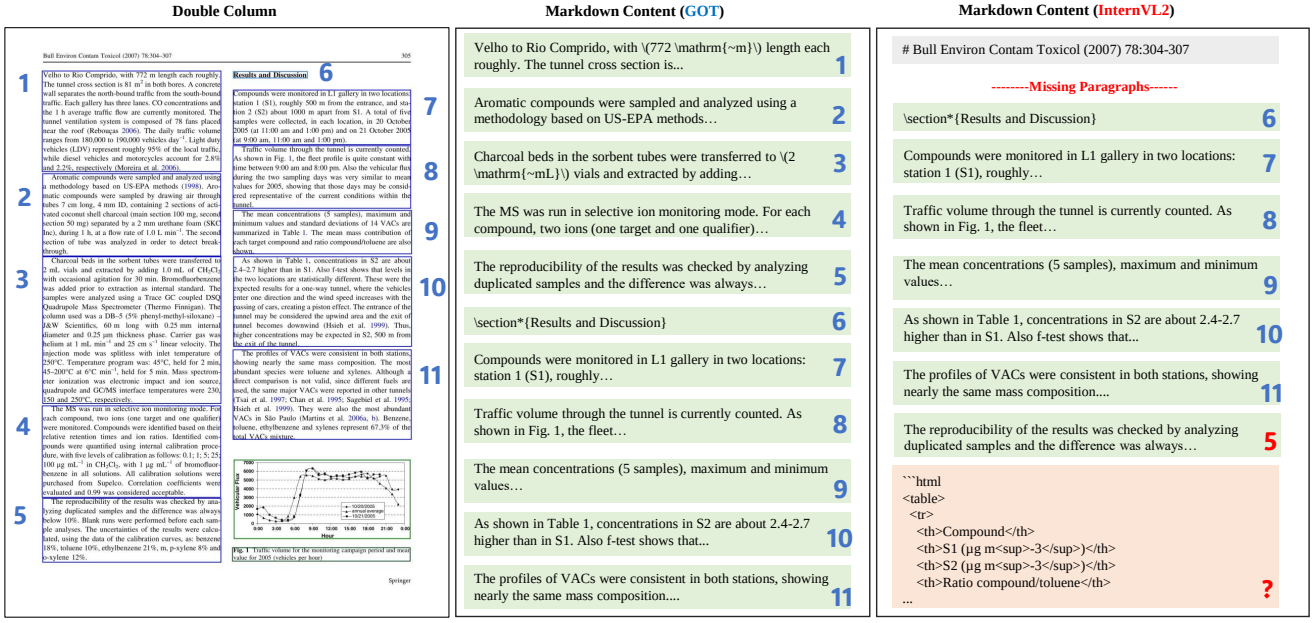

Figure S22. The Good Model Result and Bad Model Result for Double Column Pages.

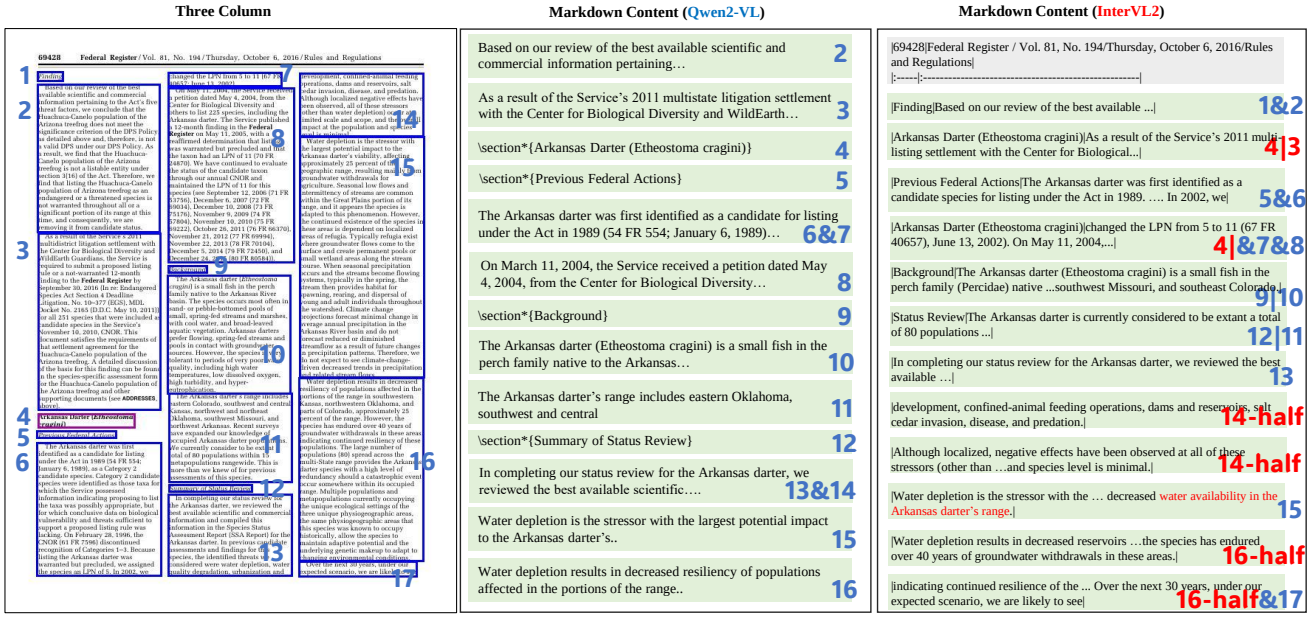

Figure S23. The Good Model Result and Bad Model Result for Three Column Pages.

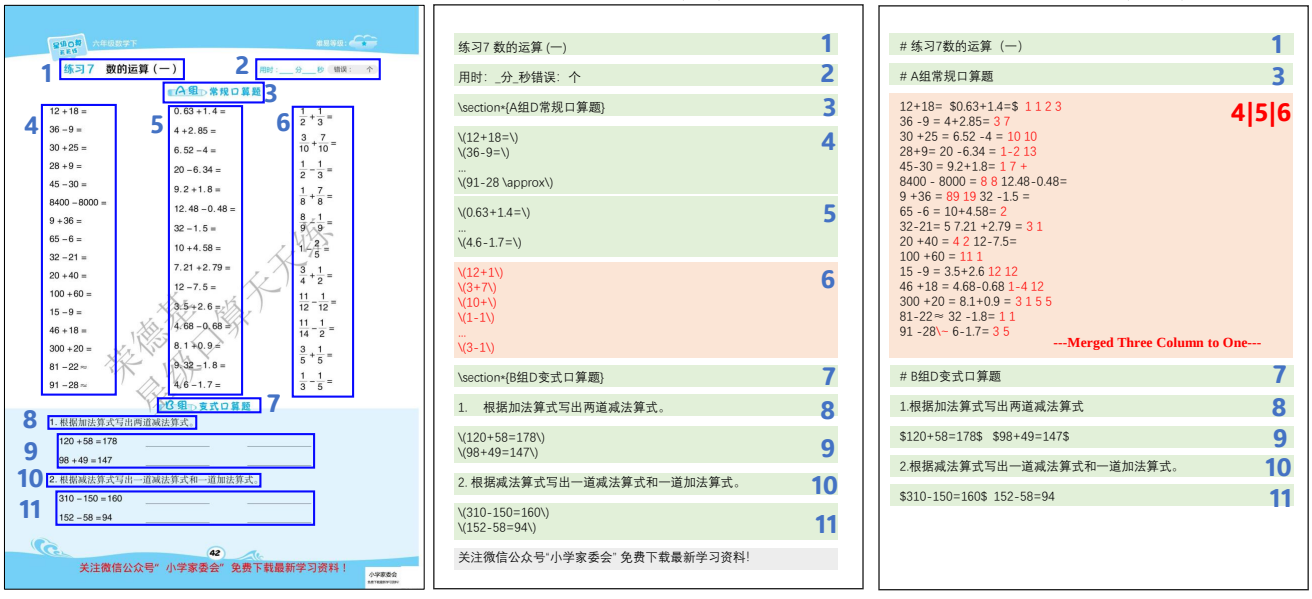

Figure S24. The Good Model Result and Bad Model Result for Complex Layout Pages.

Chinese

办公

宏观经济环境对办公资产的影响仍在持续，全球空置率达到两位数。利率上调抬高了收购和建设的债务成本，并对潜在回报率造成下行压力。随着建筑物等级成为获得资本和提升资产财务表现越来越重要的决定因素，短期内融资将面临更大挑战。

我们预计，在包括部分亚洲重点城市、地段优越以及现代化和高质量建筑群所在的地区，办公资产需求将保持旺盛，并购交易也将最为活跃。尽管到目前为止，大多数地方员工回归办公室工作的速度慢于预期，但业主们依然对日益增长的回归趋势抱有信心。

在欧洲，建筑物按规定必须达到一定能效，这一法规调整刺激了市场对优质资产的需求。例如，从2023年（荷兰）和2030年（英国）起，办公楼必须拥有能源绩效证书（EPC）C级或以上。随着越来越多的公司致力于实现去碳化，提出明确的净零目标，出租方也做出相应调整，因此，对于采用绿色科技、配备专门设施以改善租户体验的新型办公空间的需求随之上升。

Markdown Content (MinerU)

办公

宏观经济环境对办公资产的影响仍在持续，全球空置率达到两位数。利率上调抬高了收购和建设的债务成本，并对潜在回报率造成下行压力。随着建筑物等级成为获得资本和提升资产财务表现越来越重要的决定因素，短期内融资将面临更大挑战。

我们预计，在包括部分亚洲重点城市、地段优越以及现代化和高质量建筑群所在的地区，办公资产需求将保持旺盛，并购交易也将最为活跃。尽管到目前为止，大多数地方员工回归办公室工作的速度慢于预期，但业主们依然对日益增长的回归趋势抱有信心。

在欧洲，建筑物按规定必须达到一定能效，这一法规调整刺激了市场对优质资产的需求。例如，从2023年（荷兰）和2030年（英国）起，办公楼必须拥有能源绩效证书（EPC）C级或以上。随着越来越多的公司致力于实现去碳化，提出明确的净零目标，出租方也做出相应调整，因此，对于采用绿色科技、配备专门设施以改善租户体验的新型办公空间的需求随之上升。

Markdown Content (InternVL2)

办公

宏观经济环境对办公资产的影响仍在持续，全球空置率达到两位数。利率上调将提高了改建或建设的债务成本，并对潜在回报率造成下压力。随着政策收紧，政府收紧的财政政策将导致经济放缓，短期内资本市场面临更大的挑战。

我们预计，在地区部分亚洲重点城市，地段优越以及现代化和质量建筑的办公资产将成为活跃。尽管到目前为止，大多数地区的员工已返回办公室工作的速度慢于预期，但尽管理解的需求仍然强劲。

在欧洲，建筑物规定必须达到一定能效，这一法规调整刺激了市场对优质资产的需求。例如，从2023年（荷兰）和2030年（英国）的起，办公建筑必须达到A级或B级能效认证。EPIC（英国）和Sofidy（法国）等公司致力于实现去碳化，提出明确的净零目标，出租方也做出相应调整，因此，对于采用绿色科技、配置专门设施以改善建筑体验的新型办公空间的需求随之上升

。

Figure S25. The Good Model Result and Bad Model Result for Text Language in Chinese.

English

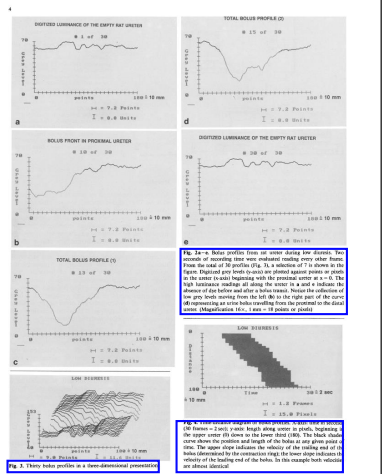

Markdown Content (Mathpix)

DIGITIZED LUMINANCE OF THE EMPTY RAT URETER

\[
\begin{array}{l}
H=7.2 \text { Points } \\
I=8.8 \text { Units } \\
\end{array}
\]

Fig. 2a-e. Bolus profiles from rat ureter during low diuresis. Two seconds of recording time were evaluated reading every other frame. From the total of 30 profiles (Fig. 3), a selection of 7 is shown in the figure. Digitized grey levels (y-axis) are plotted against points or pixels in the ureter (x -axis) beginning with the proximal ureter at \(\mathrm{x}=0 \). The high luminance readings all along the ureter in a and \(\mathbf{e} \) indicate the absence of dye before and after a bolus transit. Notice the collection of low grey levels moving from the left (b) to the right part of the curve (d) representing an urine bolus travelling from the proximal to the distal ureter. (Magnification \(16 \times, 1 \mathrm{~mm}=18 \) points or pixels)

Miss Fugre 3 caption

Fig. 4. Time-distance diagram of bolus profiles. X-axis: time in seconds (30 frames \(=2 \mathrm{sec} \)); y-axis: length along ureter in pixels, beginning in the upper ureter (0) down to the lower third (180). The black shaded curve shows the position and length of the bolus at any given point of time. The upper slope indicates the velocity of the trailing end of the bolus (determined by the contraction ring); the lower slope indicates the velocity of the leading end of the bolus. In this example both velocities are almost identical

Markdown Content (InternVL2)

 # DIGITIZED LUMINANCE OF THE EMPTY RAT URETER
#1 of 30
- H = 7.2 Points
- I = 8.8 Units

 # BOLUS FRONT IN PROXIMAL URETER
#10 of 30
- H = 7.2 Points
- I = 8.0 Units

 # TOTAL BOLUS PROFILE (1)
#13 of 30
- H = 7.2 Points
- I = 8.6 Units

 # DIGITIZED LUMINANCE OF THE EMPTY RAT URETER
#38 of 30
- H = 7.2 Points
- I = 8.4 Units

 # TOTAL BOLUS PROFILE (2)
#15 of 30
- H = 7.2 Points
- I = 8.2 Units

 # LOW DIURESIS
- H = 9.0 Points
- I = 11.6 Units

 # LOW DIURESIS
- H = 1.2 Frames
- I = 15.0 Pixels

 # Fig. 2a-e
Bolus profiles from rat ureter during low diuresis. Two seconds of recording time were evaluated reading every other frame. From the total of 30 profiles (Fig. 3), a selection of 7 is shown in the figure. Digitized grey levels (x-axis) are plotted against points or pixels in the ureter (y-axis) beginning with the proximal ureter at x = 0. The high luminescence (x-axis) readings all along the ureter indicate the absence of dye before and after bolus transit. Notice the collection of dye (grey level) representing an urine bolus leaving from the right proximal to the distal ureter. (Magnification 16x, 1 mm = 18 points or pixels)

 # Fig. 3
Thirty bolus profiles in a three-dimensional presentation

 # Fig. 4
Time-distance diagram of bolus profiles. X-axis: time in seconds (30 frames = 2 sec); y-axis: length along ureter in pixels, beginning in the upper ureter (0) down to the lower third (180). The black shaded curve shows the position and length of the bolus at any given point of time. The upper slope indicates the velocity of the trailing end of the bolus (determined by the contraction ring); the lower slope indicates the velocity of the leading end of the bolus. In this example both velocities are almost identical

Figure S26. The Good Model Result and Bad Model Result for Text Language in English.

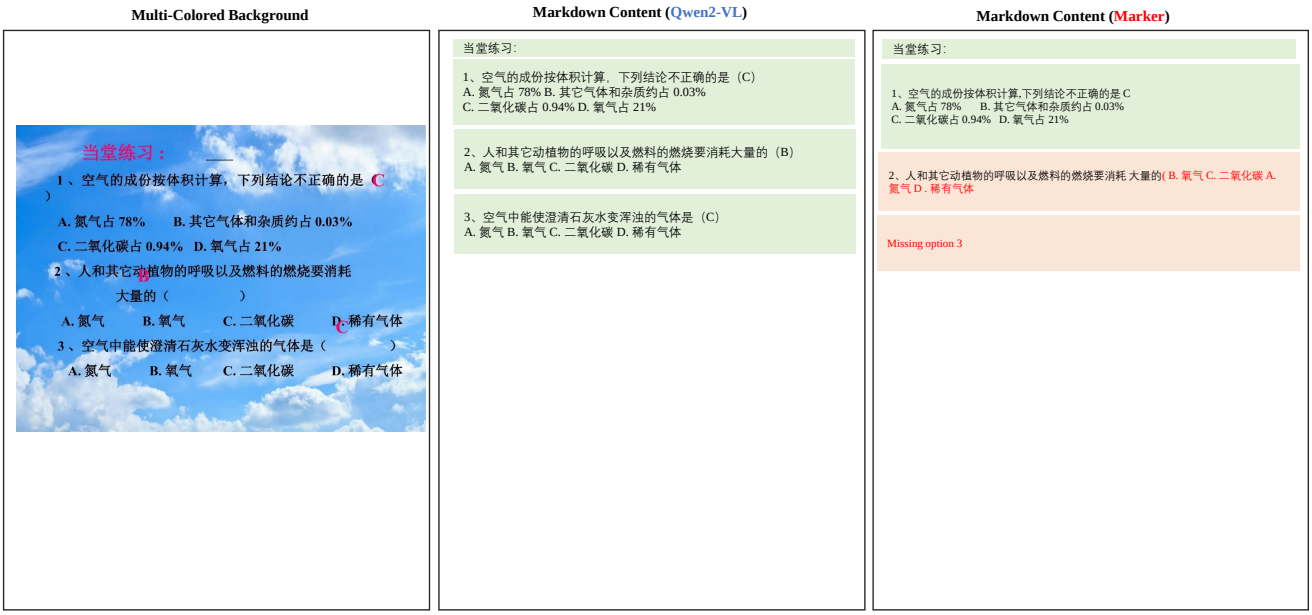

Figure S27. The Good Model Result and Bad Model Result for Text with Colorful Background.

Figure S28. The Bad Model Result for Text with Rotation.

Three Line Table

企业类型	目的	模式和特点	优势	典型企业
云服务提供商	• 以物联网为抓手带动上层应用服务业绩增长	• 目前多以提供底层计算资源、提供应用使能平台为主	• 在互联网领域中积累了丰富的技术、商业、生态优势经验 • 底层IaaS能力突出、共性技术能力提炼	阿里云、腾讯云、百度云、亚马逊AWS IoT等
通信领域厂商	• 获得流量业务收入，战略布局物联网，把握新增市场机遇	• 多以连接管理、应用使能为平台主要功能服务为主	• 在连接管理平台具有绝对优势，具有全球通用连接能力	电信运营商、通信设备厂商，中国电信天翼物联、如中国移动ONENet、中国联通物联网平台、华为云IoT等
软件系统服务商	• 解决内部开发效率的问题，优化产品服务	• 以应用开发平台为主要服务内容为主	• 擅长软件设计、生产、管理、运维等服务，具备丰富的行业软件开发及服务经验	紫光云、广联达筑联等
垂直领域传统厂商	• 利用自身对行业的理解与经验，打造垂直型平台，实现传统企业的转型升级	• 垂直专业领域的物联网平台	• 深刻的行业理解和行业技术、对行业有深度应用，拥有行业数据和客户资源	西门子、工业富联、美的M-Smart等企业
初创企业	• 看好物联网未来的发展潜能	• 目前阶段很多初创型平台企业多以SaaS解决方案公司的形式存在	• 拥有与选定细分行业相关的软件、硬件经验 • 服务延伸到通用型平台厂商难以触及的细分领域，形成错位竞争	涂鸦智能、云智易、机智云、艾拉物联等

Good Model Result (RapidTable)

企业类型	目的	模式和特点	优势	典型企业
云服务提供商	层应用服务业绩增长	以物联网为抓手带动上· 目前多以提供底层计算资源、提供应用使能平台为主	在互联网领域中积累了丰富的技术、商业、生态优势经验 ·底层IaaS能力突出、共性技术能力提炼	阿里云、腾讯云、百度云、亚马 逊AWSIoT等
通信领域厂商	获得流量业务收入，战略布局物联网，把握新 增市场机遇	、多以连接管理、应用使能为 平台主要功能服务为主	·在连接管理平台具有绝对优势，具有全球 通用连接能力	电信运营商、通信设备厂商，中 国电信天翼物联、如中国移动 ONENet、中国联通物联网平台、华为云IoT等
软件系统服务商	解决内部开发效率的问题，优化产品服务	·以应用开发平台为主要服务 内容为主	·擅长软件设计、生产、管理、运维等服务，具备丰富的行业软件开发及服务经验	紫光云、广联达筑联等
垂直领域传统厂商	利用自身对行业的理解 与经验，打造垂直型平 台，实现传统企业的转 型升级	垂直专业领域的物联网平台	深刻的行业理解和行业技术、对行业有深 度应用，拥有行业数据和客户资源	西门子、工业富联、美的M- Smart等企业
初创企业	看好物联网未来的发展 潜能	目前阶段很多初创型平台企 业多以SaaS解决方案公司的 形式存在	拥有与选定细分行业相关的软件、硬件经 验 服务延伸到通用型平台 厂商难以触及的细 分领域，形成错位竞争	涂鸦智能、云智易、机智云、艾 拉物联等

Bad Model Result (PaddleOCR)

企业类型	目的	模式和特点	优势
云服务提供商	目前多以提供底层计算资源、提供应用使能平台为主	在互联网领域中积累了丰富的技术、商业、生态优势经验 ·底层IaaS能力突出、共性技术能力提炼	阿里云、腾讯云、百度云、亚马 逊AWSIoT等
通信领域厂商	获得流量业务收入，战略布局物联网，把握新 增市场机遇	·多以连接管理、应用使能为 平台主要功能服务为主 ·在连接管理平台具有绝对优势，具有全球 通用连接能力	电信运营商、通信设备厂商，中 国电信天翼物联、如中国移动 ONENet、中国联通物联网平台、华为云IoT等
软件系统服务商	解决内部开发效率的问 题，优化产品服务	·擅长软件设计、生产、管理、运维等服务 具备丰富的行业软件开发及服务经验 ·以应用开发平台为主要服务	紫光云、广联达筑联等
垂直领域传统厂商	·利用自身对行业的理解 与经验，打造垂直型平 台，实现传统企业的转 型升级	深刻的行业理解和行业技术、对行业有深 度应用，拥有行业数据和客户资源 垂直专业领域的物联网平台	西门子、工业富联、美的M- Smart等企业
初创企业	看好物联网未来的发展 潜能	拥有与选定细分行业相关的软件、硬件经 验 服务延伸到通用型平台厂商难以触及的细 分领域，形成错位竞争 ·目前阶段很多初创型平台企 业多以SaaS解决方案公司的	涂鸦智能、云智易、机智云、艾 拉物联等

Figure S29. The Good Model Result and Bad Model Result for Three Line Frame Table.

Table No Frame

HEX ROW	WINTER MINUS	AXIAL TILT FACTOR	AXIAL TILT TEMP MINUS IN WINTER	NIGHTTIME MINUS	ORBIT ECC MINUS	LOWEST TEMP FOR HEX ROW
1	-45	0.5	-23	101	0.0	-113
2	-45	0.75	-34	101	0.0	-130
3	-45	1	-45	101	0.0	-147
4	-45	1	-45	101	0.0	-153
5	-45	1	-45	101	0.0	-159
6	-45	1	-45	101	0.0	-165
7	-45	1	-45	101	0.0	-171
8	-45	1	-45	101	0.0	-177
9	-45	1	-45	101	0.0	-183
10	-45	1	-45	101	0.0	-189
11	-45	1	-45	101	0.0	-195

Good Model Result (PaddleOCR)

			AXIAL TILT			LOWEST
HEX	WINTER	AXIAL TILT	TEMP MINUS	NIGHTTIME	ORBIT ECC	TEMP FOR
ROW	MINUS	FACTOR	IN WINTER	MINUS	MINUS	HEX ROW
1	-45	0.5	-23	101	0.0	-113
2	-45	0.75	-34	101	0.0	-130
3	-45	1	-45	101	0.0	-147
4	-45	1	-45	101	0.0	-153
5	-45	1	-45	101	0.0	-159
6	-45	1	-45	101	0.0	-165
7	-45	1	-45	101	0.0	-171
8	-45	1	-45	101	0.0	-177
9	-45	1	-45	101	0.0	-183
10	-45	1	-45	101	0.0	-189
11	-45	1	-45	101	0.0	-195

Bad Model Result (Qwen2VL-7B)

HEX ROW	WINTER MINUS	AXIAL AXIAL FACTOR	TILT TILT IN	TEMP WINTER	MINUS MINUS	LOWEST NIGHTTIME ORBIT ECC TEMP FOR
1	-45	0.5	-23	101	0.0	-113
2	-45	0.75	-34	101	0.0	-130
3	-45	1	-45	101	0.0	-147
4	-45	1	-45	101	0	-153
5	-45	1	-45	101	0 .	-159
6	-45	1	-45	101	00	-165
7	-45	1	-45	101	0,0	-171
8	-45	1	-45	101	0 , 0	-177
9	-45	1	-45	101	0 0	-183
10	-45	1	-45	101	0 o	-189
11	-45	1	-45	101	050	-195

Figure S30. The Good Model Result and Bad Model Result for No Frame Table.

Rotate

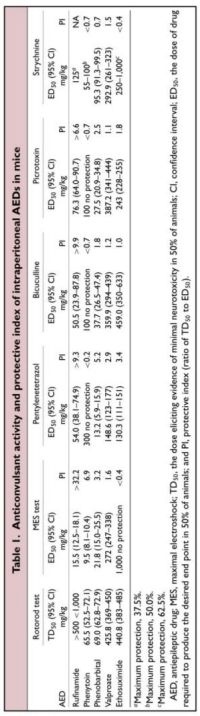

Table 1. Anticonvulsant activity and protective index of intraperitoneal AEDs in mice

AED	Rotorod test TD50 (95% CI) mg/kg	MES test ED50 (95% CI) mg/kg	MES test PI	Pentylenetetrazol ED50 (95% CI) mg/kg	Pentylenetetrazol PI	Bicuculline ED50 (95% CI) mg/kg	Bicuculline PI	Picrotoxin ED50 (95% CI) mg/kg	Picrotoxin PI	Strychnine ED50 (95% CI) mg/kg	Strychnine PI
Rufinamide	>500 <1,000	15.5 (12.5–18.1)	>32.2	54.0 (38.1–74.9)	>9.3	50.5 (23.9–87.8)	>9.9	76.3 (64.0–90.7)	>6.6	125[a]	NA
Phenytoin	65.5 (52.5–72.1)	9.5 (8.1–10.4)	6.9	300 no protection	<0.2	100 no protection	<0.7	100 no protection	<0.7	15–100[a]	<0.7
Phenobarbital	69.3 (60.4–77.2)	21.8 (17.2–25.5)	3.2	75.2 (61.7–85)	1.2	33.7 (26.4–41.4)	1.8	72.2 (60.2–84.8)	1.1	95.3 (76.1–99.5)	0.7
Valproate	425.8 (369–450)	272 (247–338)	1.6	148.6 (123–177)	2.9	359.9 (294–439)	1.2	387.2 (341–444)	1.1	292.9 (261–323)	1.5
Ethosuximide	440.8 (383–485)	1,000 no protection	<0.4	130.3 (111–151)	3.4	459.0 (350–633)	1.0	243 (228–335)	1.8	250–1,000[c]	<0.4

[a]Maximum protection, 37.5%.
[b]Maximum protection, 50.0%.
[c]Maximum protection, 62.5%.
AED, antiepileptic drug; MES, maximal electroshock; TD_{50}, the dose eliciting evidence of minimal neurotoxicity in 50% of animals; CI, confidence interval; ED_{50}, the dose of drug required to produce the desired end point in 50% of animals; and PI, protective index (ratio of TD_{50} to ED_{50}).

Good Model Result (StuctEqTable)

	Rotorod test TD 95% CI mg/kg > 500 1000	MES test mg/kg	Pentylenetrilol ED-95% C mg/kg	Buculine ED 05 (95% C) mg/kg		Strychnine ED 08 95% C) mg/kg		
Rufimane	> 500 1000	155.12 18-18	> 540 (38.1-49.3)	> 50.23 (23.87)		> 125%	NA	
Phenoyliron	65.52 -77.21	9.18 10-14)	300 no protection	90 no protection	> 70.2			
Phenobarbil	692.6 -72.9)	21.15 -25.5	132 (5.19)	377 (26.47)	> 50 (23.4)	55 -100%	95.9 (1.39)	> 0.7
Valproate	4258 (369 -450)	272 (247.38)	1486 (123 -177)	1.6	> 2.9	292.9 (26.12 -31.23)	12.1	1.5
Ethosuximide	4408 (338 -485)	1,000 no protection	1303 (111 -15)	< 0.4	314	4590 (350 -633)	1.8	< 0.4
a Maximum	protection							
b Maximum	37.5%							
c ADE, antilepileprotectic, drug, MES,	50.5%							
AED, antilepileprotectic, drug, the desired end point in 50% of animals; and PI, protective PI, TD 0.5 to 0.50, and PI, protective index of TD to 0.50.	56.2%							

Bad Model Result (GOT-OCR)

Error pred: <|im_end|>};

Figure S31. The Good Model Result and Bad Model Result for Rotated Table.

Table Contain Formula

名称	氧化亚铁	氧化铁（俗称铁红）	四氧化三铁（俗称磁性氧化铁）
化学式	FeO	Fe_2O_3	Fe_3O_4
颜色、状态	黑色粉末	红棕色粉末	黑色晶体
铁的价态	+2 价	+3 价	+2、+3 价
水溶性	均不溶于水		
与非氧化性酸反应	$FeO+2H^+ = Fe^{2+}+H_2O$	$Fe_2O_3+6H^+ = 2Fe^{3+}+3H_2O$	$Fe_3O_4+8H^+ = Fe^{2+}+2Fe^{3+}+4H_2O$
与 H_2、CO、Al 等反应	$FeO+H_2 \xrightarrow{\triangle} Fe+H_2O$	$Fe_2O_3+3CO \xrightarrow{高温} 2Fe+3CO_2$	$3Fe_3O_4+8Al \xrightarrow{高温} 9Fe+4Al_2O_3$

Good Model Result (Qwen2VL-7B)

名称	氧化亚铁	氧化铁（俗称铁红）	四氧化三铁（俗称磁性氧化铁）
化学式	FeO	Fe O	Fe O
颜色、状态	黑色粉末	红棕色粉末	黑色晶体
铁的价态	+2 价	+3 价	+2、+3 价
水溶性	均不溶于水	均不溶于水	均不溶于水
与非氧化性酸反应	FeO+2H =Fe² +H O	Fe O +6H =2Fe³ +3H O	Fe O +8H =Fe² +2Fe³ +4H O
与 H 、CO、Al 等反应	FeO+H =Fe+H O	Fe O +3CO=2Fe+3CO	3Fe O +8Al=9Fe+4Al O

Bad Model Result (InternVL2-8B)

名称	氧化亚铁	氧化铁（俗称铁红）	四氧化三铁（俗称磁性氧化铁）	化学式	颜色、状态	铁的价态
				FeO	黑色粉末	+2 价
				Fe_2O_3	红棕色粉末	+3 价
				Fe_3O_4	黑色晶体	+2、+3 价
水溶性						均不溶于水
与非氧化性酸反应	$FeO + 2H^+ = Fe^{2+} + H_2O$	$Fe_2O_3 + 6H^+ = 2Fe^{3+} + 3H_2O$	$Fe_3O_4 + 8H^+ = Fe^{2+} + 2Fe^{3+} + 4H_2O$			
与 H_2、CO、Al 等反应	$FeO + H_2 = Fe + H_2O$	$Fe_2O_3 + 3CO = 2Fe + 3CO_2$	$3Fe_3O_4 + 8Al = 9Fe + 4Al_2O_3$		高温	

Figure S32. The Good Model Result and Bad Model Result for Table with Formula.